Bull. Min. Res. Exp. (2016) 153:63-90

Bulletin of the Mineral Research and Exploration

http://bulletin.mta.gov.tr

DIAGENETIC HISTORY OF THE ROCK UNITS OF BOZKIR UNIT CONTROLLED BY THE TRIASSIC RIFTING, BOZKIR-KONYA

Hüseyin YALÇIN[a*], Ömer BOZKAYA[b] and Mine TAKÇI[c]

[a]*Cumhuriyet University, Dept. of Geol. Eng., 58140 Sivas, Turkey*
[b]*Pamukkale University, Dept. of Geol. Eng., 20070 Denizli, Turkey*
[c]*Cumhuriyet University, Graduate School of Sciences, 58140 Sivas, Turkey*

Research Article

Keywords:
Taurus Belt, Extensional basin, Phyllosilicate, Mineralogy and Geochemistry

ABSTRACT

The Bozkır Unit representing the northern edge of the Taurus Belt comprises, from bottom to top, three distinct structural entities; the Upper Triassic pre-rift (Korualan Group), the Upper Triassic-Upper Cretaceous syn-rift (Huğlu Group) and the Jurassic-Cretaceous Boyalı Tepe Group as to their structural settings. The Korualan Group is represented by the alternations of carbonate (limestone, dolomitic limestone, dolomite) with radiolarite and chert intercalations and clastic rocks (sandstone, siltstone, mudstone, shale). The Huğlu Group is made up of volcanic (basalt, andesite) and pyroclastic (tuffaceous sandstone) rocks including radiolarite, limestone and clastic rock (sandstone, siltstone, shale) intercalations. The Boyalı Tepe Group is completely made of carbonate rocks. The carbonate-silisiclastic-volcanogenic rocks of the Bozkır Unit contain carbonate (calcite, dolomite), quartz, feldspar (plagioclase, anorthoclase), phyllosilicate (illite, chlorite, mixed-layered illite-chlorite / I-C, chlorite-vermiculite / C-V, chlorite-smectite / C-S, rare smectite), augite, hematite, analcime and heulandite in order of abundance. On the basis of illite Kübler Index data; Korualan and Huğlu Group reflect low grade diagenetic, high grade diagenetic and high grade diagenetic-anchizonal characteristics, respectively. The illite/micas of the pre-rift units and units related to the rifting have muscovitic, and phengitic and seladonitic compositions, respectively. The distributions of chondrite-normalized trace and rare earth element (*REE*) contents in illites present similar trends for Korualan ve Huğlu groups, but the quantities of these elements slightly increase in the Huğlu Group. $\delta^{18}O$–δD isotopic compositions of water forming the illite minerals are different than that of sea water and are found to be between the Eastern Mediterranean Meteoric Water (EMMW) and magmatic water compositions. It also shows that temperature of the water forming illite minerals varies from low to high values. The findings from the rocks of Bozkır Unit suggest that pre- and syn-rift units have different mineralogical-petrographic and geochemical properties. The younger units within the rift due to extension and crustal thinning related to rifting must have been exposed in higher diagenetic conditions by more burial and heat with respect to older units on the edges.

Received: 05.02.2016
Accepted: 29.03.2016

1. Introduction

In diagenetic-low grade metamorphic rocks, the mineralogical parameters such as; the mineral assemblages, illite crystallinity, *b* cell dimension of white K-micas, phyllosilicate polytypes and etc. (Bozkaya and Yalçın, 1996) are extensively used in world literature for the last 30 years at an increasing rate in order to establish the geological evolution of related rocks (Frey, 1987; Liou et al., 1987; Merriman and Frey, 1999; Merriman and Peacor, 1999). The studies, which are about autochthonous and allochthonous units especially in Taurus belt in our country (Bozkaya and Yalçın, 1997*a*, 1997*b*, 1998, 2000, 2004, 2005, 2010; Bozkaya et al., 2002, 2006*a*) provided significant contributions for the interpretation of tectono-stratigraphic units. Besides; the opening/extension related to rifting and the following inversion has significantly influenced the diagenetic/metamorphic evolution of the rocks with detailed mineralogical-petrographic studies carried out successively in Triassic (Antalya Unit) and Eocene (Maden Group) diagenetic/metamorphic deposits in western Taurus and the southeastern Anatolian regions (For example; Bozkaya et al., 2006*b*; Bozkaya and Yalçın, 2010).

The Bozkır Unit, which consists of rock block and slices in different dimensions and appear as mélange deposited between Triassic-Cretaceous time intervals, forms the northernmost unit of the Taurus Belt (Özgül, 1997, Alan et al., 2014). It also comprises sedimentary and volcanic rocks related with the Triassic rifting similar to the Alakırçay Nappe of the Antalya Unit. The Triassic rifting restricting the northern (Bozkır

* *Corresponding Author: Hüseyin YALÇIN yalcin44@gmail.com*
http://dx.doi.org/10.19111/bfmre.266051

Unit) and southern (Antalya Unit) edges of the Taurus Platform is an important geological event in terms of the evolution of the northwest Gondwana and represents the opening of the northern and southern branches of the Neotethys and the beginning of the Alpine cycle (Göncüoğlu, 2010).

In this study, it was aimed at investigating the detailed mineralogical and geochemical characteristics of Triassic-Cretaceous sedimentary and volcanic rocks of the Bozkır Unit in Bozkır-Hadim (Konya) region where the most typical outcrops of the Bozkır Unit are observed. Thus, the establishment of the degree of diagenesis-metamorphism related to rifting will give significant contributions for the interpretation of Lower Mesozoic evolution of the northern edge of the Taurus Belt; and so for the geology of Turkey. In other words; it will be possible to correlate other Taurus units which were previously studied by the authors, with the degree of diagenesis-metamorphism of the Antalya Unit (Alakırçay nappe) by means of findings that will be obtained from the Bozkır Unit.

2. Regional Geology

The Central Taurus carries the explicit characteristics, and it is one of the most significant sections of the Taurus Belt. It has been the subject of many investigations since 1940, and it has been understood that it had consisted of rock unit assemblages, which are tectonically in contact with each other, showing continuity along belt and reflecting different environmental conditions of the region in terms of stratigraphy, metamorphism and structural characteristics (Blumenthal, 1944, 1947, 1951, 1956; Özgül, 1971, 1976, 1984; Brunn et al., 1971; Özgül and Arpat, 1973; Monod, 1977; Gutnic et al., 1979). These assemblages, which are emplaced successively and gain the characteristic of a different tectono-stratigraphic unit as a result of horizontal displacements reaching hundreds of kilometers by means of Senonian and Lutetian movements were named as; Geyik Dağı Unit, Aladağ Unit, Bolkar Dağı Unit by Özgül (1976), Bozkır Unit, Alanya Unit and Antalya Unit (Figure 1).

Among the units, which can be observed both in Eastern and Western Taurus, it is known that the Bozkır Unit located in north and the Antalya Unit located in south consist of deep marine deposits and ophiolites; however, the Bolkar Dağı, Aladağ, Alanya and the Geyik Dağı units mainly comprise shelf type clastic and carbonated rocks, and they are all overlain by allochthonous units of the Geyik Dağı Unit which is relatively autochthonous (Özgül, 1976). Considering the stratigraphic and relative structural settings of the tectono-stratigraphic units of the Central Taurus, it is adopted that; all units formed a single platform a couple of thousand kilometers wide at the end of Cambrian-Early Triassic (Scythian) interval (Özgül, 1997). At the beginning of Anisian; this platform entered the rifting and re-rifting processes at sections corresponding to the Antalya Unit in south and the Bozkır Unit in north of this platform (Antalya Nappes; Marcoux, 1978) (Figure 2). It is also accepted that the northern and southern branches of the Tethys Ocean, which is represented by the Antalya and Bozkır units, were closed in Senonian and accordingly; the Bozkır Unit overlies the Bolkar Dağı and Aladağ units in north, and the Alanya Unit overlies the Antalya Unit in south (Özgül, 1984). It is claimed that "Dipsiz Göl Ophiolitic Complex" consisting of ophiolite, pelagic limestone and divergent turbidites was derived in Late Senonian-Early Tertiary interval between the Geyik Dağı and Aladağ units in north. It is also asserted that an short-lived basin might have developed and as being related with the closure of this basin in Lutetian, the Aladağ and Bolkar Dağı units overlain by the Bozkır Unit moved from north to south and the Antalya Unit overlain by the Alanya Unit moved from south to north to each other and overlaid the Geyik Dağı Unit (Özgül, 1997).

3. Stratigraphy and Lithology

In addition to sedimentary, volcano-sedimentary and volcanic rocks deposited in Triassic-Cretaceous time interval, the Bozkır Unit, which consists of blocks and slices in different sizes of rocks of the much older units (Özgül, 1976), appears as a big mélange and has been the subject to several studies. The outcrops of the unit, which remain at different sections outside the study area on Taurus, are known as; the Western Lycian Nappes (Graciansky, 1967), the Eastern Lycian Nappes around Korkuteli (Brunn et al., 1971), Beyşehir-Hoyran Nappe around Beyşehir-Seydişehir in the Central Taurus (Gutnic et al., 1979), Ophiolitic sequence around Hadim-Bozkır (Özgül, 1971), Schist-Radiolarite formation in Karaman (Konya) region (Blumenthal, 1956), and the nappes consisting of Triassic units in Hadim-Taşkent region are known as; the Bucakışla tectonic slice and Huğlu Group (Alan et al., 2014).

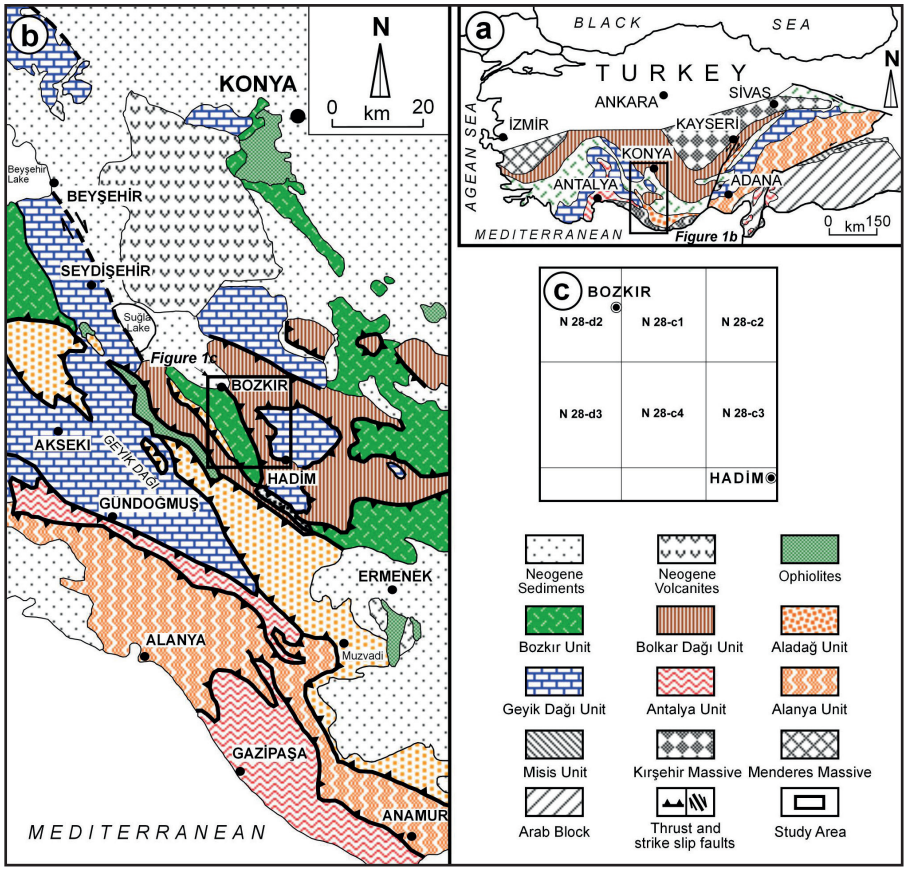

Figure 1- a) Tectonic units of the Southern Anatolia (Göncüoğlu et al., 1997; Özgül, 1976), b) The setting in the Tauride units (Özgül, 1984) outcropped in the Tauride of the study area, c) The distribution of the study area according to the sheets.

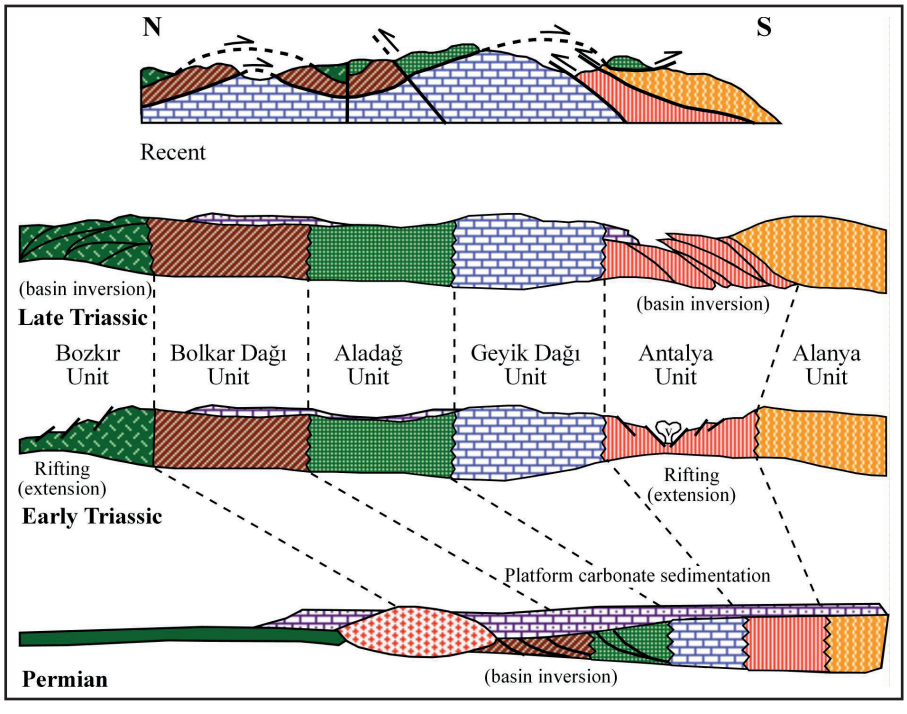

Figure 2- Schematic display of the geological evolution during the Permian-Triassic from Taurus Belt units (arranged from Özgül, 1984).

The outcrops, where units in different age intervals and lithologies in the Central Taurus in which the Bozkır Unit is located, and tectono-stratigraphic relationships were given in figures 3.1a and 3.1b, respectively. Among these; the Bozkır Unit, which consists of the subject of the study, was divided from bottom to top into units as; Upper Triassic Korualan Group (Kayabaşı formation, Başkışla Complex), Upper Triassic-Upper Cretaceous Huğlu Group (Dedemli formation, Mahmut Tepesi Limestone, Kovanlık Complex) and Jurassic-Cretaceous Boyalı Tepe Group (Soğucak Limestone/Kuztepe Limestone, Asar Tepe Limestone) units by Özgül (1997) according to recent structural settings. Besides, in the description of stratigraphic characteristics of the units Özgül (1976), Gutnic and Monod (1970), Monod (1977) and Gökdeniz (1981) have put significant contributions. Although the dominant lithology is limestone in the Mahmut Tepe Limestone among these units, it is more appropriate to name it as the Mahmut Tepe formation as it also consists of shale and siltstone intercalations. The locations of the samples collected from the Bozkır Unit and the details of the relationships between units related with the rift development were given in figure 4 with small scale geological map and field photos.

The Kayabaşı formation of the Korualan Group consists of dolomite, neritic foraminiferal limestone and shallow marine deposits containing reefal limestone, sandstone-shale intercalation with lensoidal reefal limestone at the bottom and nodular, radiolarian pelagic limestones with pelecypod shells and flintstone interlayers at the top. The formation represents the pre-rift carbonate deposition of the Bozkır Unit and has the characteristic of a sedimentary deposit which deepens towards upper layers.

Başkışla Complex is made up of shell traced (radiolarian and pelecypod) pelagic limestone, radiolarite, clastics with debris flow, andesitic blocks and from the mixture of rare green tuffs and fine grained debris flow clastics. The unit reflects the beginning of the rift and gives the image of mixture of blocks in similar characteristics (probably derived from them) with the rock units belonging to the other slices of the Bozkır Unit with dimensions reaching up to hundreds of meters. For example; green tuff and andesitic volcanic rocks, which are partially observed in the complex, show resemblance with the volcanics of the Dedemli formation; the pelagic limestones with radiolarite interlayers with the Mahmut Tepe formation and the neritic limestones resemble to the lower parts of the Boyalı Tepe formation.

The Dedemli formation of the Huğlu Group, which is synchronously or directly related with rifting, begins with the clastic layer consisting of unsorted limestone and pebbly, blocky debris flow accumulations with sandy-clayey groundmass. Then the section which is exclude the rare limestone and clastic intercalations is completely formed by tuff, tuffite, diabase and few andesitic submarine volcanics. Pale-dark green tuff and tuffites reflecting the volcanic products related with opening and/or extension (Andrew and Robertson, 2002) form the dominant rock type of the formation which can easily be recognized on the field.

The Mahmut Tepesi formation is fully formed by the pelagic limestone, which is flintstone interlayered and thin shale intercalated in lower parts, and ends up with red and thin layered micritic level located at the uppermost part. The unit exhibits a view reflecting the basin deepening with syn-sedimentary faults on the Dedemli formation (Figure 4).

The Kovanlık Complex, in addition to mainly pebble and small blocks, consists of radiolarite, pelagic and neritic carbonate (limestone, dolomite), volcanic slices and clastic rock (shale, sandstone) layers with heights reaching hundreds of meters. Spilitic volcanics are in different colors (black, dark brown, dark green) and easily disintegrate and occasionally show amygdaloidal pillow structures partly with zeolite infillings. In basaltic-andesitic volcanics, seldom high grade crystallized, dark red radiolarite and limestone patches are observed.

The Boyalı Tepe Group is composed of cream, dark red-pink, medium-thick layered, partly much fossilliferous neritic limestones with thin flintstone interlayers.

4. Material and Method

Total of 183 mineral and rock samples were collected in the study area. After the samples were washed, they were subjected to thin-section, crushing-pulverization-sieving, clay separation, X-ray diffraction (XRD) and optical microscopy (OM) processes in the Mineralogy-Petrography and Geochemical Research Laboratories (MİPJAL) of the

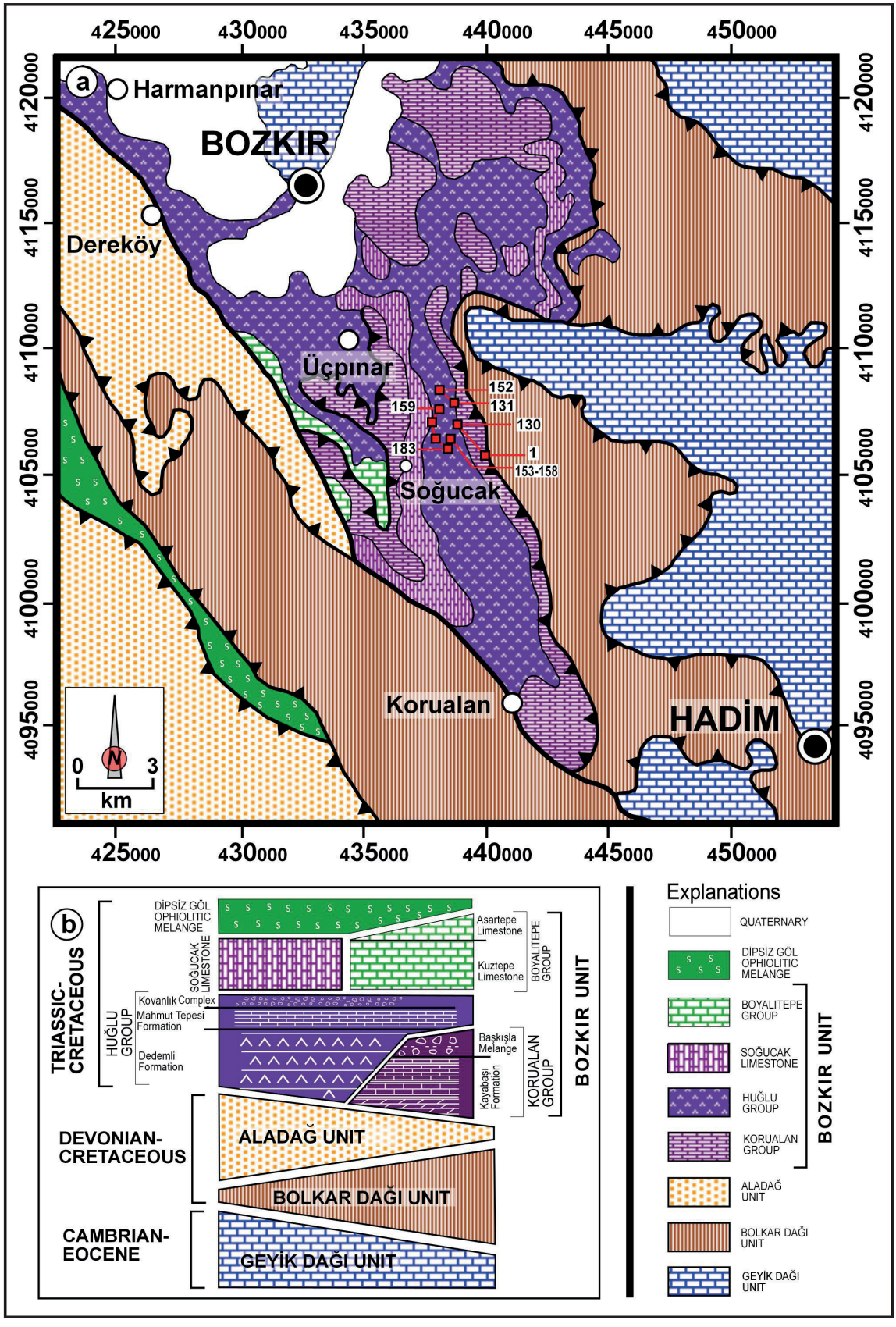

Figure 3- a) Geology map of the study area (adapted from MTA, 2002), b) The relative settings of the Units (arranged from Özgül, 1997).

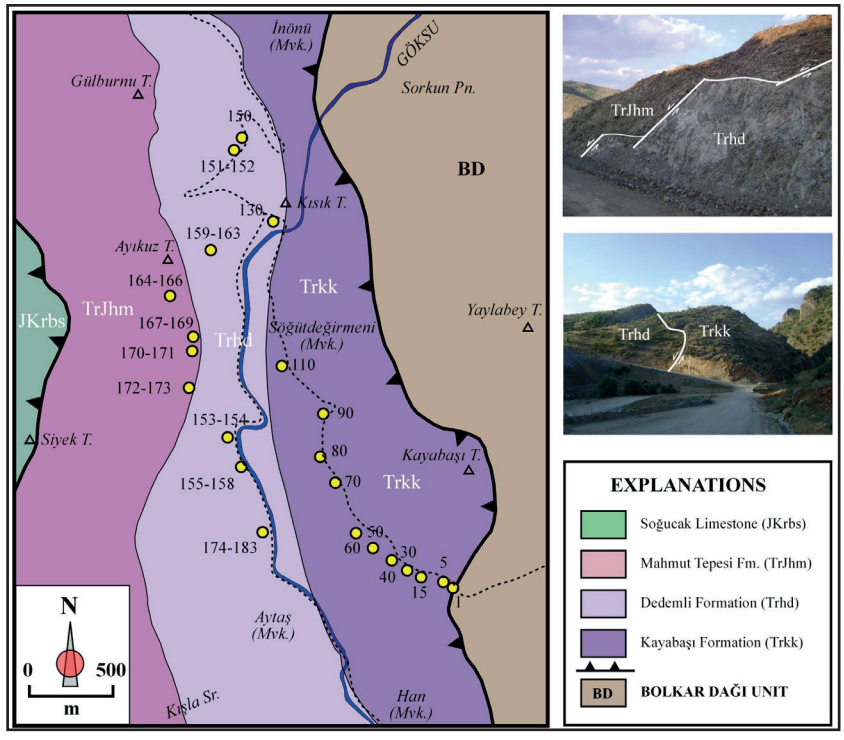

Figure 4- Geology map of the study area in the vicinity of sampling locations and field views showing rifting (arranged from MTA, 2002 and field observations).

Geological Engineering Department of the Cumhuriyet University (C.U.). The scanning electron microscope-secondary electron (SEM-SE), back scattered electron microscope (SEM-BSE) views and the energy dispersion spectrometer (EDS) analyses were carried out in the Laboratories of Scientific Research Center (Centro de Instrumentación Científica) of the Granada University (Universitad de Granada, Spain). For the major element analyses of illites, the trace and rare earth element (REE) analyses and the oxygen-hydrogen isotope geochemistry of illites; inductively coupled plasma spectrometer (ICP), inductively coupled plasma – mass spectrometer (ICP-MS) and the thermal ionization mass spectrometer (TIMS) were used, respectively in the Activation Laboratories Ltd. (Actlabs) in Canada.

The optical microscopy studies were performed by the transmitted light binocular polarized microscope (Nikon). By this method, the compositions and textural characteristics of the rocks were defined and described, and their alteration products were studied.

The XRD method was used in order to determine the whole rock mineralogical compositions (XRD-WR) of the rocks, the clay fraction (XRD-CF) and polymorphic changes in minerals, which are too small in grain size to study under the optical microscope (OM).

The samples used in XRD studies were first crushed by a hammer in 3-5 cm pieces and by the Fritisch brand jaw crusher into grains less than 5 mm, then pulverized by silicon carbide bowl grinder of the same brand for 10-30 minutes considering their hardness's. The dust materials obtained in this way were made ready to analysis after putting into nylon bags and stickered. XRD analyses were performed by DMAX IIIC model X-ray diffractometer of Rigaku (Anode = Cu (CuKα = 1.541871Å), Filter = Ni, Voltage = 35 kV, Current = 15 mA, Goniometer speed = 2°/min., Paper speed = 2cm/min., Time constant = 1 sec, Slits = 1° 0.15 mm 1° 0.30 mm, record interval = 2θ = 5-35°). As a result of XRD analyses, the whole rock and clay size components of the samples were defined (< 2μm) and semi-quantitative percentages were estimated based on the non-standard method (Brindley, 1980). The mineral intensity factors in XRD-WR and CF estimations and the reflections were measured in mm. In this method, the dolomite and kaolinite were taken as reference for the whole rock and clay fraction from the ethylene glycolation

pattern (Yalçın and Bozkaya, 2002). Quartz was used as the internal standard in measuring *d* distances. The description of clay minerals was mainly made according to (00l) basal reflections.

In phyllosilicate/clay bearing rocks, the process of separation of these minerals from the others are basically formed by chemical solution (the removal of non-clay fraction), centrifugation-decantation and leaching, suspension-sedimentation-siphoning-centrifugation and bottling. This process was accelerated by adding Calgon in cases when there had not been any siphoning process. The centrifugation was performed by the centrifuge of the Heraeus Sepatech brand Varifuge 3.2 S model with 5600 rev./min and 200 cc capacity metal codes. From each clay muds, the plastering or three oriented glass slides were prepared in the form of suspension for the ones that have swelled and cracked and then they were dried in room temperature. Clay fraction diffractograms were obtained by untreated-N (air-dried), ethylene glycolated-EG (to leave under ethylene glycol vapor in desiccator for 16 hours under the temperature of 60°C) and heating-F (4 hours heating under the temperature of 490°). During scanning, the goniometer speed and the recording interval were adjusted as 1°/min and 2θ=2-30° (error rate ± 0.04°).

In the polytype determination of pure or nearly pure illite minerals, the distinguishing peaks suggested by Bailey (1980 and 1988) and J.C.P.D.S. (1990) were used. For the detection of polytype, recording interval with 2θ = 16-36° and goniometer speed of 2°/min. were utilized.

Three dimensional morphological view studies were carried out on carbon coated samples which randomly broken into 1cm^3 sizes for SEM-SE analysis. Semi-quantitative EDS analyses were also utilized in minerals descriptions. For two-dimensional texture and mineral chemistry studies, the rock slices were cut and one of their sides were polished, and made ready to analysis coated with carbon. First; the mineral description and textural relationships were examined by BSE on polished sections, then EDS analyses were carried out in suitable points and areas. For EDS analyses; the Oxford INCA system was used and instrumental conditions were adjusted as 20 kV in voltage and with a probe size of 250 pA.

The results of oxygen and hydrogen isotopes have the accuracy of ± 0.2 ‰ and were estimated based on Vienna Standard Mean Ocean Water (V-SMOW). For stable isotope geochemistry and the description of isotopic standards, the processes of analyses were given by Clayton and Mayeda (1963) and by O'Neil (1986) in detail. Details of the analysis method and instrumental detection limits were given on the official web site of the firm (http://www.actlabs.com/).

5. Mineralogy-Petrography

5.1. Optical Microscopic Studies

Among lithologies forming the Korualan Group, the orthochem micritic and sparitic calcite and/or dolomites are seen in carbonate rocks, and the extraclastics are constituted by quartz, feldspar (mainly plagioclase), clay, opaque minerals (mainly hematite) and muscovite in order of abundance. In some samples, the fossil shell fragments and allochem components of radiolarian were encountered. According to Folk (1974); these rocks were defined as micrite, lithomicrite, micrite with quartz, micrite with radiolaira, dolomicrite, oomicrite, microsparite, sparite, sparite with quartz and dolomite, dolomicrosparite, dolosparite with calcite and dolosparite.

Sparites consist of coarse calcite minerals similar to crystallized limestones (Figure 5a). In oolites, the multi concentric oolites with lamellae are observed (Figure 5b). At the center of some oolites, the quartz minerals are encountered. Fossil remnants, radiolarians and fine grained opaque minerals are seen in bonding material.

In pores of the micrites; the euhedral rhombohedral and zone textured calcites (Figure 5c), in pores of the dolosparites; the euhedral rhombohedral dolomites are observed (Figure 5d). Dolosparites occasionally exhibit a gel texture and dolomites are surrounded by opaque minerals (hematite) in places.

The components of the siliciclastic rocks are constituted in order of abundance by monocrystalline and polycrystalline quartz, feldspar (mainly plagioclase), rock fragments (mainly metamorphic), mica minerals (muscovite and biotite), chlorite and opaque minerals (mainly hematite). However, tourmaline and zircon minerals are seldom observed. The bonding material is represented by the clay matrix and carbonate cement (calcite and dolomite). Siliciclastic rocks were

described as sandstone, siltstone, mudstone and shale according to grain size and mineral contents. The sandstones among these were defined according to quartz (Q), feldspar (F), rock fragments (L) and matrix (M) content (for M < % 15 Folk, 1974; for M > % 15 Pettijohn, 1975). These rocks were named as; quartz sandstone, arkose, litharenite and feldspathic litharenite (M<%15) or as lithic greywacke (M>%15) (Figure 5e). The sandstones, from mineralogical and textural points of view, are mainly mature-submature and of some are submature-immature. However, in pores of cherts with calcite and/or dolomite, the gel textured chalcedonic quartz (Figure 5f) is observed.

Volcanic rocks, which constitute one of the most widespread lithologies of the Huğlu Group exhibit three different textures as; hypocrystalline porphyritic, vitrophyric porphyritic and aphanitic-amygdaloidal. The pale colored components in these rocks are formed by plagioclase, and dark colored components are formed by augite, biotite and occasionally by opaque minerals (mainly hematite). The matrix is mainly represented by volcanic glass and plagioclase microlites in occasion. These rocks were described as basalt and andesite according to Streckeisen (1978) classification considering the primary magmatic composition and their textural characteristics.

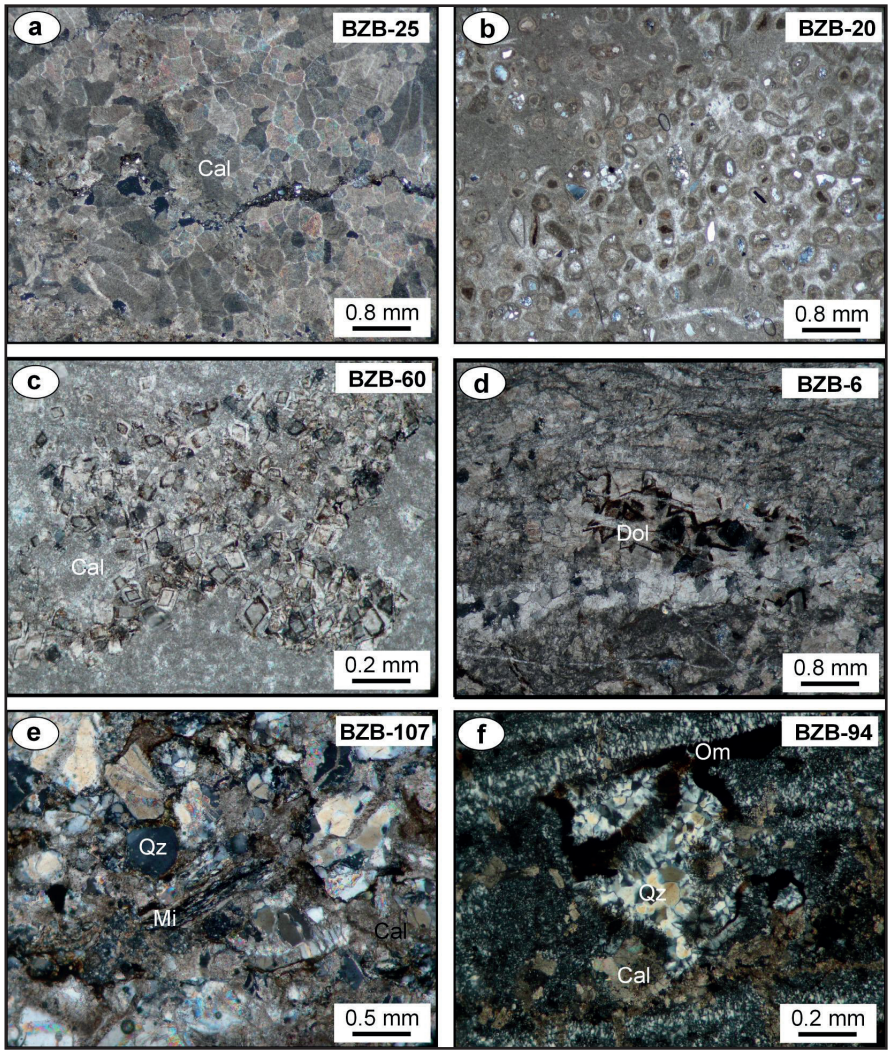

Figure 5- Optical microscopic views of carbonate rocks from the Korualan Group (crossed polarized light; Cal: Calcite, Dol: Dolomite, Qz: Quartz, Mi: Mica, Om: Opaque minerals), a) Sparites including coarse calcite crystals, b) Oomicrites with quartz and fossils, c) Micrites including euhedral, rhombohedral and zoned calcites within the pores, d) Dolosparites including euhedral, rhombohedral and zoned dolomite crystals within the pores and partly gel texture, e) Angular, monocrystalline and polycrystalline quartz within the calcite cement and detrital micas in the quartz sandstones, f) Chalcedonic quartz and gel texture within the pores of coarse-grained dolomitic chert.

In matrix and pores of the rocks, frequently the silicification, argillization and chloritization and partly zeolitization (analcime and heulandite/clinoptilolite) are observed (Figure 6a-b).

Pyroclastic rocks are vitroclastic in texture and contain quartz, plagioclase, opaque minerals and volcanic rock fragments. In bonding material, mainly the silicified and/or chloritized volcanic glass and carbonate minerals are encountered (Figure 6c-d). Pyroclastic rocks were defined as tuffaceous sandstone (tuffite) according to grain size and the ratios of pyroclastic (volcanic glass, pumice, crystal and volcanic rock fragments) / (epiclastic + chemical + organic) components (Schmid, 1981).

In carbonate rocks, also the silicified and/or carbonate textured radiolarian fossils are frequently encountered.

5.2. Electron Microscope Studies

SEM-SE (three dimensional) and SEM-BSE (two dimensional) views on polished surface of the rocks of the Bozkır Unit were given in figures 7 and 8, respectively.

Illite and chlorites are observed among quartz and feldspar grains in the form of flaky and plumy-like groups in shale (BZB-17) and mudstone (BZB-45) lithologies, which possess illite + quartz + calcite + feldspar + chlorite assemblage, of the Korualan Group (Figure 7a-b). Illite and chlorite minerals in authigenic or diagenetic recrystallized origin form the main components of the rock orientation. In the altered volcanic rock sample (BZB-100), which has illite + chlorite + quartz + feldspar + calcite paragenesis in the Huğlu Group, the illites are plumy-like and chlorites are flaky and form a distinctive orientation (Figure 7c). Among the coarse grain components in siltstone sample of the Huğlu Group (BZB-182), the completely authigenic fibrous

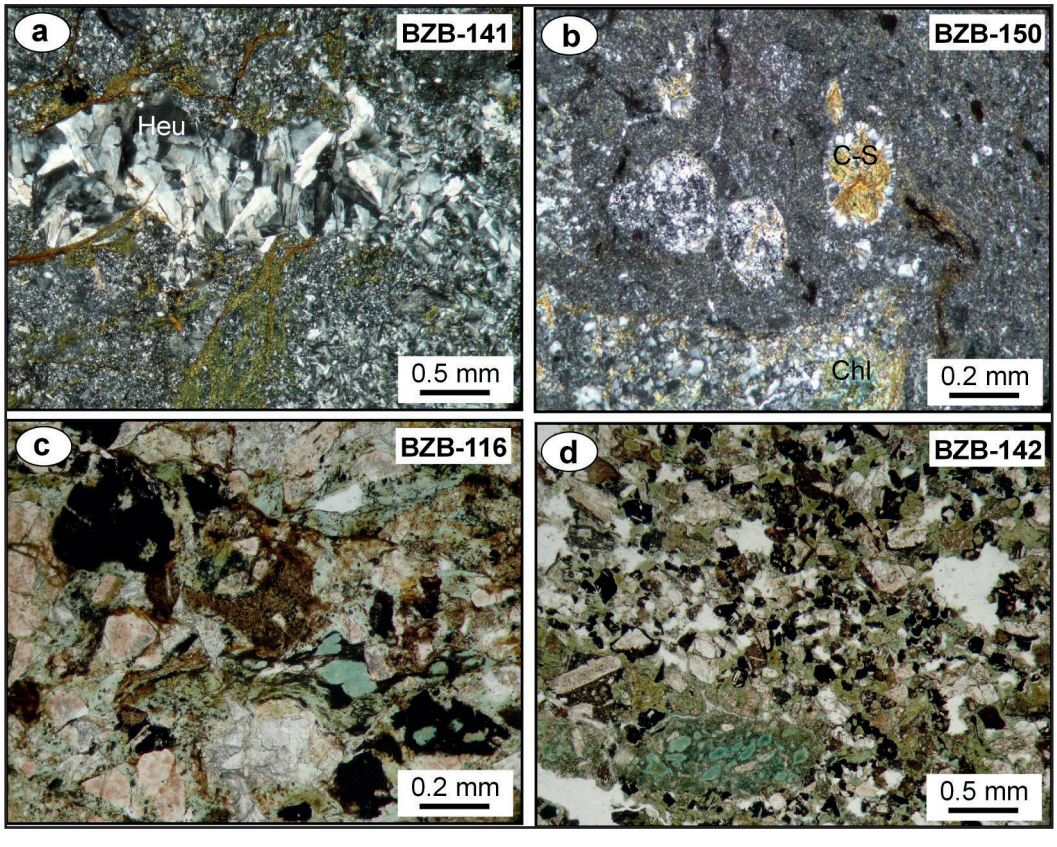

Figure 6- Optical microscopic views of Huğlu Group rocks (a-b: crossed polarized light, c-d: plane polarized light; Heu: Höylandit, Chl: Chlorite, C-S: Mixed-layered chlorite-smectite), a) Heulandites/clinoptilolites within the matrix and/or pores in the altered andesites, b) Chlorite and mixed-layered chlorite-smectite (C-S) within the matrix and/or pores in the altered andesites, c) Chloritization, carbonatization and volcanic rock fragments in the vitroclastic textured tuffaceous sandstones, d) Chloritizations in the vitroclastic textured tuffaceous sandstones.

I-C minerals are also observed in addition to feather and flaky illite and chlorites (Figure 7d).

The back scattered electron (BSE) microscope views of sandstone and mudstone samples of the Korualan Group have shown that the phyllosilicates, which are the main components of the orientation, are represented by fine grained illite and chlorite formations infilling the spaces of calcite, quartz and feldspar grains in addition to coarse dendritic micas (Figure 8a-b). In addition to silicate and carbonate minerals in mudstones, the framboidal pyrites, which formed as a result of probable bacterial reduction, were also observed (Figure 8b). In altered volcanic rock sample of the Huğlu Group, the pale gray-white iron rich components (chlorite, hematite) increase and also the orientation related with the burial can be observed in addition to the volcanic texture (Figure 8c). In siltstone sample, in which the clastic texture is dominant, the coarse grained platy mica (dark gray) and chlorites (pale gray) form a distinctive orientation (Figure 8d). The authigenic illite and chlorites are observed in the form of fine grained constituents which infill the grains.

5.3. X-Ray Diffraction Studies

5.3.1. Whole Rock and Clay Fraction Studies

In siliciclastic and carbonate rocks of the Korualan Group; the quartz, feldspar, clay and hematite minerals, and calcite and dolomite minerals are observed as dominant minerals, respectively in order of abundance. In siliciclastic rocks of the unit, mainly the illite, partly chlorite, smectite and mixed-layered I-S constitute clay minerals (Figure 9a-b).

The volcanic components of volcanic and pyroclastic rocks of the Huğlu Group in order of abundance are composed of feldspar (mainly plagioclase), augite, hornblende, biotite and hematite, and the post volcanic components are constituted by quartz, clay, calcite, dolomite, analcime and goethite. The mineralogy of silicilastic and carbonate rocks is similar to that of the Korualan Group except for their abundances. In volcanic-pyroclastic rocks of the unit (Dedemli Formation), the clay minerals are represented mainly by illite, chlorite, partly smectite and by the mixed-layered I-S. The deep marine silicified rocks

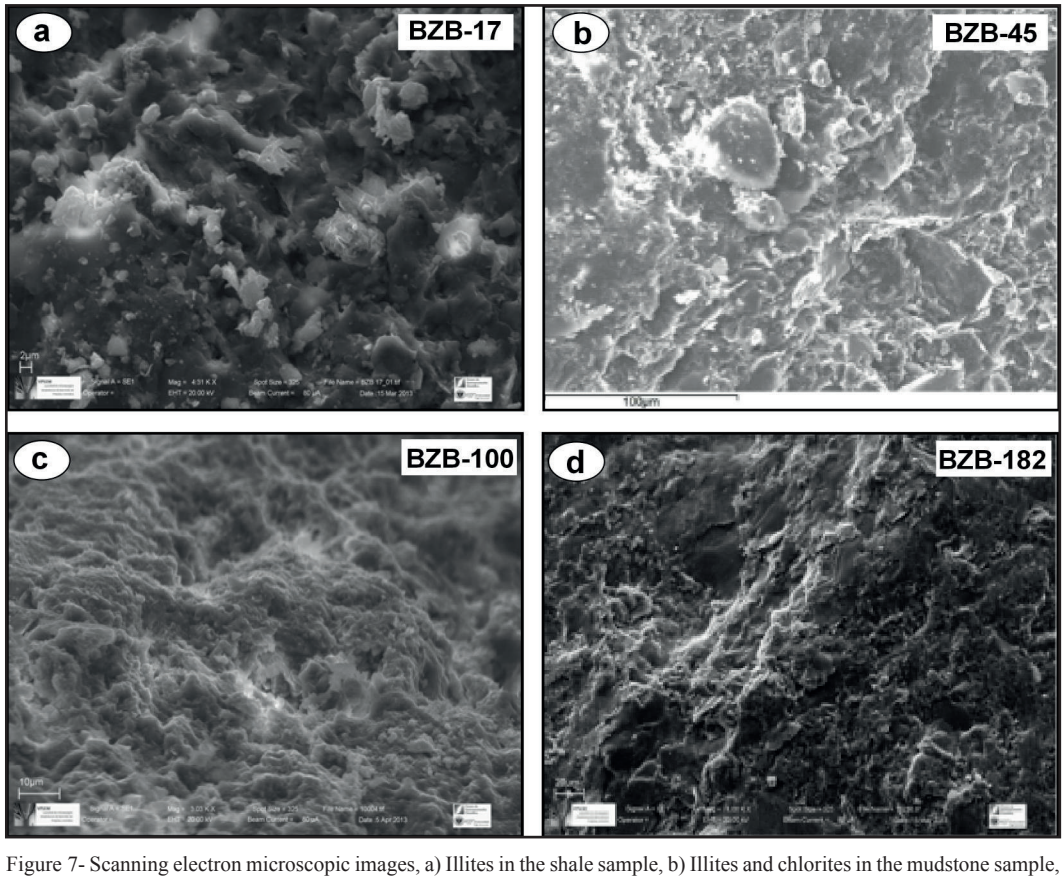

Figure 7- Scanning electron microscopic images, a) Illites in the shale sample, b) Illites and chlorites in the mudstone sample, c) Illites and chlorites in the altered volcanic sample, d) Illite, chlorite and mixed-layered illit-chlorite (I-C) in the siltstone sample.

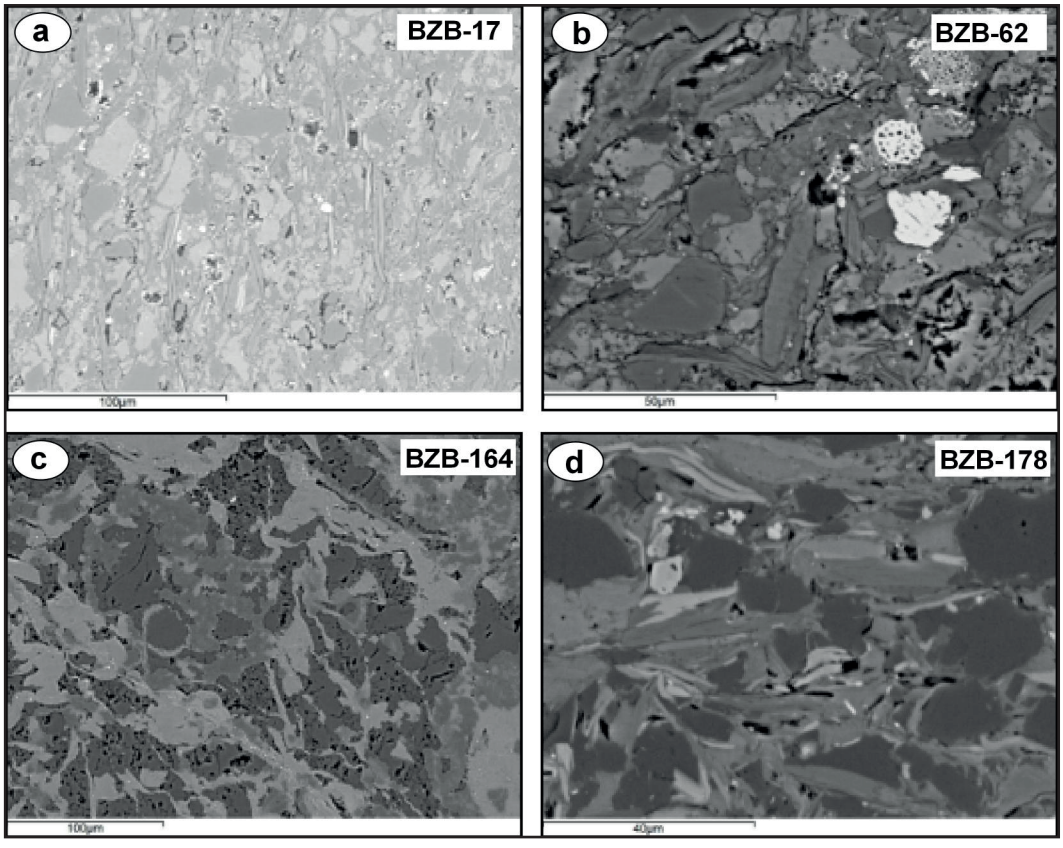

Figure 8- Backscattered electron microscopic images, a) Orientations of the illites in the shale sample, b) Detrital mica, authigenic illite and framboidal pyrite occurrences in the mudstone sample, c) Fine-grained hematites in the altered volcanic sample, d) Orientations of the micas and chlorites in the siltstone sample.

(Mahmut Tepesi Formation) contain C-V and C-S in addition to illite, chlorite and I-S minerals.

5.3.2. The Crystal Chemistry Studies of Phyllosilicates

The "crystallinity" values of illite and chlorite minerals of the Bozkır Unit obtained by the calibration of peak values (FWHM) in semi-height measured by means of WINFIT program were given in table 1. For illite and chlorite minerals the Kübler index (KI:Kübler, 1968) and the Arkai index (AI: Arkai, 1991; Guggenheim et al., 2002) were used, respectively.

The crystallinity measurement values for units were assessed in KI-I(002)/(001) diagram (Figure 10), and correspond with the Kayabaşı formation 1.48-2.31 $\Delta^o2\theta$ (mean 1.82 $\Delta^o2\theta$. low grade diagenesis), the Dedemli formation 0.54-0.81 $\Delta^o2\theta$ (mean 0.63 $\Delta^o2\theta$, high grade diagenesis) and the Mahmut Tepesi formation 0.35-0.76 $\Delta^o2\theta$ (mean 0.53 $\Delta^o2\theta$, anchizone and high grade diagenesis) values.

The relationship between the crystallinity degree (KI) and peak intensity ratio (Ir), which were determined in different lithologies of the Bozkır Unit, was given in figure 11. Accordingly; the Kayabaşı formation, the Dedemli formation and the Mahmut Tepesi formation reflect low grade diagenesis, high grade diagenesis and anchizone-high grade diagenesis, respectively.

The illites, which give a peak at 10 Å in N- and EG-patterns and do not show any extension in EG-pattern, might contain smectite even in fewer amounts. In case when illites contain smectite layer both the peak intensity of (003) reflection increases and 10 Å peak width decreases in EG-pattern. The peak intensity ratio suggested by Srodon (1984) ($Ir=I(003/001)_{air\text{-}dried}/I(003/001)_{glycolated}$) is one of the most widely used methods and Ir>1 means that illites contain smectite interlayer. Using the diagram generated according to crystallinity and Ir values of illites by Eberl and Velde (1989), it was assessed that illites had contained an expandable layer (smectite) (Figure 11).

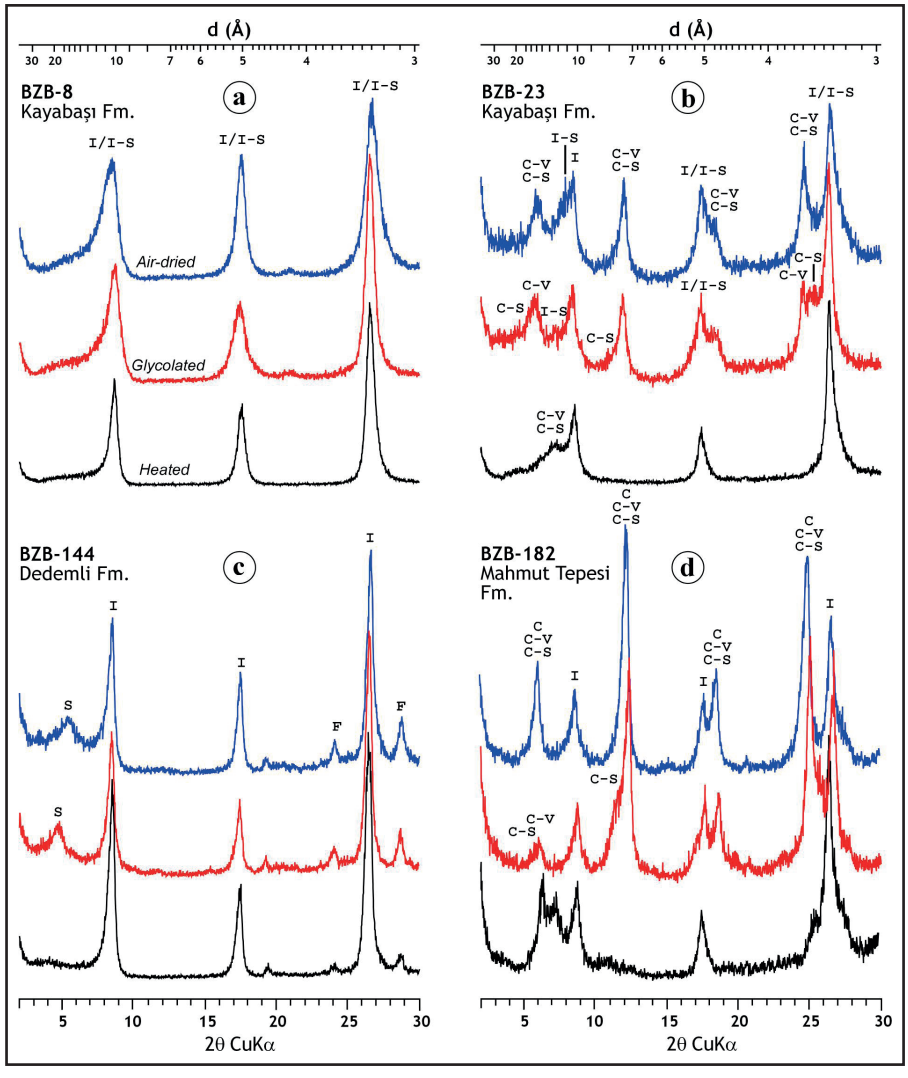

Figure 9- XRD-CF patterns of the Bozkır Unit rocks, a) Illite / I-S, b) Illite + I-S +C-V + C-S, c) Illite + Smectite, d) Illite + Chlorite + C-V + C-S.

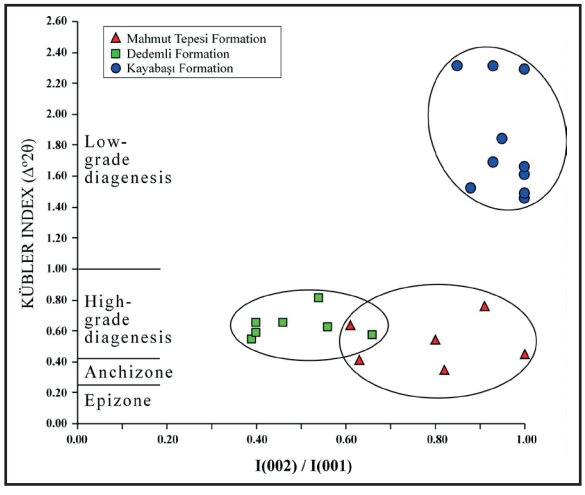

Figure 10- The distribution of KI-I(002)/(001) peak intensity ratios in the K-micas from the Bozkır Unit rocks.

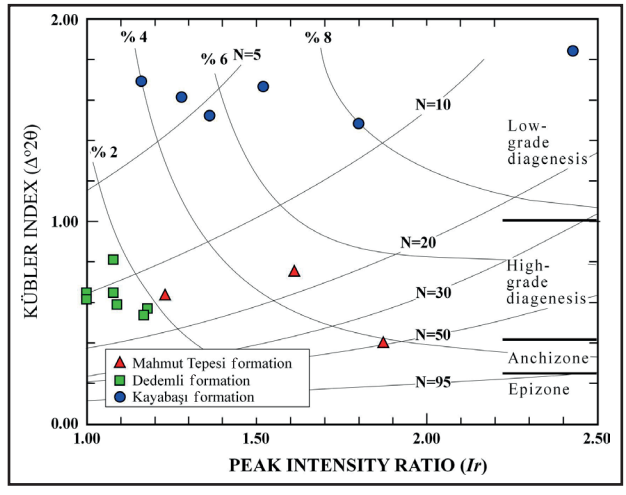

Figure 11- The relationship between expandable layer content (S %) and crystallite size of K-micas in the KI-[$I_{(003)}/I_{(001)N}$] / [$I_{(003)}/I_{(001)G}$] diagram (Eberl and Velde, 1989) from the Bozkır Unit rocks.

Thus, the expandable layer components of illites (smectite %) is in between 4-8 % in the Kayabaşı formation, less than 2 % in the Dedemli formation and between 2-5 % in the Mahmut Tepesi formation.

The crystalline size of illites, according to the formula (N_{001}=8.059/β; β=1.038949 x KI-0.8250323) suggested by Merriman et al. (1990), are 3-6 nm in the Kayabaşı formation (mean 5 nm), 11-17 nm (mean 14 nm) in the Dedemli Formation and 11-29 nm (mean 19 nm) in the Mahmut Tepesi formation (Table 1). The crystallite sizes of illites in KI-Ir diagram show a similarity with the values estimated from Merriman et al. (1990) (Figure 11).

The polytype and d_{060} measurements made in pure or nearly pure illites of the Kayabaşı Formation were given in figure 12. The illites mainly form from $2M_1$ and $1M_d$ polytypes, and a sample far from rifting (BZB-8) contains $1M$ polytype. According to d_{060} values (1.4996-1.5007 Å, mean 1.5002 Å), the illites are completely dioctahedral in composition (Octahedral Fe+Mg=0.18 atom).

6. Geochemistry

6.1. Major Element Geochemistry

Illite, smectite and vermiculites are clay minerals structurally related with micas, and they are distinguished from each other by the tetrahedral-octahedral-tetrahedral (T-O-T or 2:1) interlayer cation to be potassium. The ones that resemble to muscovite are dioctahedral; and the others resembling to biotite are trioctahedral. The general formula for illite can be expressed as; $K_yAl_4[Si_{8-y.0}Al_yO_{20}](OH)_4$ and here y<2 and mostly around 1.5.

The chemical compositions of some mica minerals that should be taken into consideration in the

Table 1- The results of "crystallinite", peak intensity ratio (Ir) and crystallite size (N, mm) measurements of illite and chlorite in the Bozkır Unit.

Sample No	FWHM-I	FWHM-C	KI-I	KI-C	Ir(*)	N(**)	I(002)/I(001)
Kayabaşı Formation							
BZB-8	1.450		1.61		1.28	5	1.00
BZB-17	1.523		1.69		1.16	5	0.93
BZB-23	1.376		1.52		1.36	5	0.88
BZB-28	1.319		1.46			6	1.00
BZB-45	2.038		2.29		1.77	4	1.00
BZB-69	1.651		1.84		2.43	4	0.95
BZB-71	1.493		1.66		1.52	5	1.00
BZB-89	2.055		2.31		2.33	3	0.93
BZB-105	2.055		2.31		1.86	3	0.85
BZB-131	1.337		1.48		1.80	6	1.00
Dedemli Formation							
BZB-100	0.621		0.65		1.00	14	0.46
BZB-117	0.592		0.62		1.00	14	0.56
BZB-140	0.755		0.81		1.08	11	0.54
BZB-144	0.549		0.57		1.18	16	0.66
BZB-161	0.526		0.54		1.17	17	0.39
BZB-164	0.566		0.59		1.09	15	0.40
BZB-165	0.622		0.65		1.08	14	0.40
Mahmut Tepesi Formation							
BZB-171	0.615		0.64		1.23	14	0.61
BZB-178	0.415	0.415	0.41	0.41	1.87	23	0.63
BZB-179	0.529	0.410	0.54	0.41		17	0.80
BZB-180	0.362	0.385	0.35	0.38		29	0.82
BZB-181	0.445	0.447	0.45	0.45		21	1.00
BZB-182	0.714		0.76		1.61	11	0.91

(*) Ir = $[I(003)/I(001)_{normal}] / [I(003)/I(001)_{glycole}]$

(**) N001 (nm) = 8.059/β; β=1.038949 x KI-0.8250323

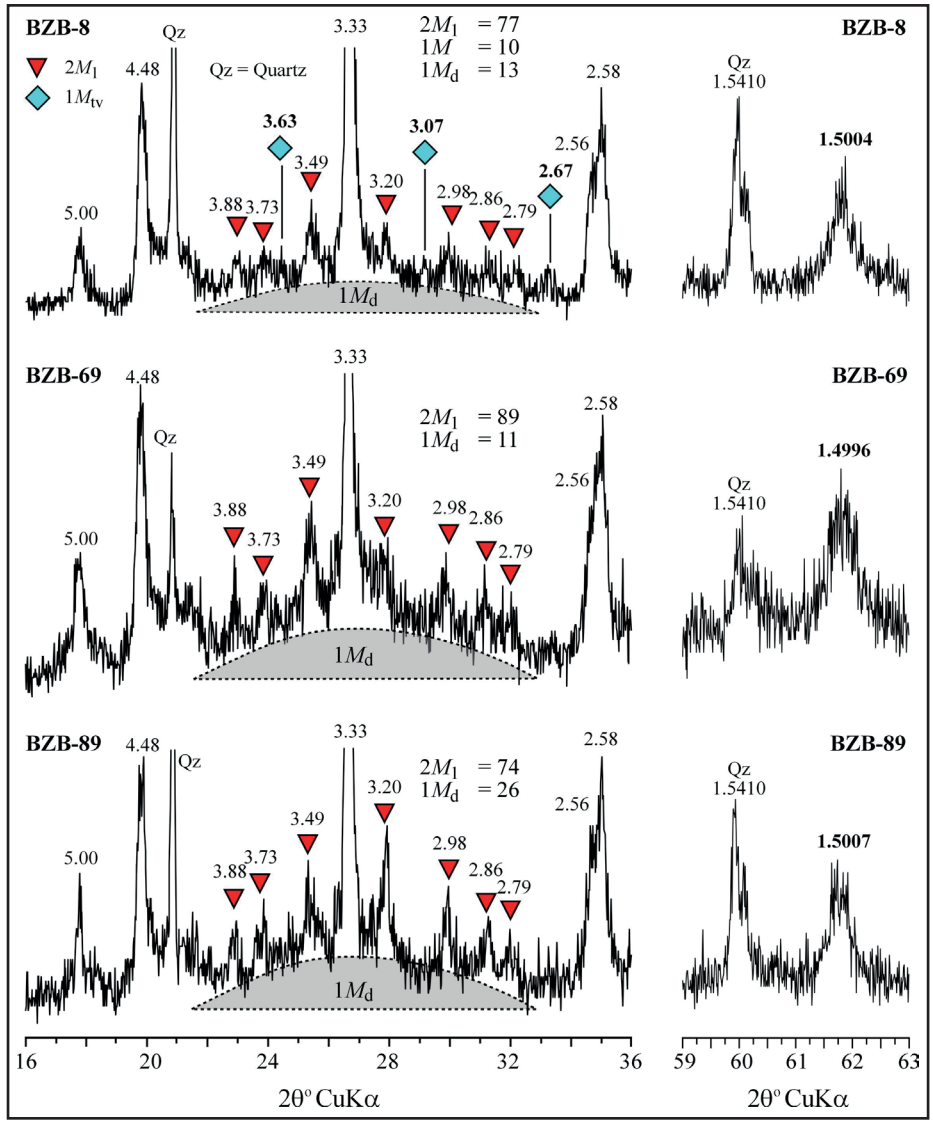

Figure 12- XRD patterns of polytypes and d_{060} values of illite in the Bozkır Unit rocks.

assessment of illites are given below. The structural and oxide formulae of theoretical muscovite and seladonite are successively; $K_2Al_4[Si_6Al_2O_{20}](OH,_F)_4$ ve $K_2O.3Al_2O_3.6SiO_2.2H_2O$ (SiO_2 45.26 %, Al_2O_3 38.40 %, K_2O 11.82 %, H_2O 4.52 %), $K_2(MgFe^{2+}Fe^{3+}{}_2)[Si_8O_{20}](OH)_4$ and $K_2O.Fe_2O_3.MgO.FeO.8SiO_2.2H_2O$ (SiO_2 54.45 %, Fe_2O_3 18.09 %, FeO 8.14 %, MgO 4.57 %, K_2O 10.67 %, H_2O 4.08 %). The structural and oxide formulae of theoretical biotite is $K_2Fe_6[Si_6Al_2O_{20}](OH)_4$ (K_2O 9.20 %, FeO 42.11 %, SiO_2 35.21 %, Al_2O_3 9.96 %, H_2O 3.52 %); and for phlogopite it is $K_2Mg_6[Si_6Al_2O_{20}](OH)_4$ (K_2O % 11.29, MgO 28.98 %, SiO_2 43.19 %, Al_2O_3 12.22 %, H_2O 4.32 %).

The major element contents of illite minerals detected by the ICP method and the structural formulae estimated based on 11 oxygen atom (Weaver and Pollard, 1973) were presented in table 2. The distribution of major oxides based on their content in illites shows nearly 50 times increase (SiO_2) and 100 times decrease (MnO) when 1 % value is taken as reference. The most distinctive difference according to samples is observed in ΣFe_2O_3, CaO and Na_2O contents.

Illites that have dioctahedral composition possess tetrahedral Al (0.04-0.49) substitution. The octahedral substitution and total octahedral cation amount related with Al, Mg, Fe, T, and Mn vary between 0.15-0.52 and 1.86-1.96, respectively. The major cation located between the interlayer is K, and its amount ranges from 0.37 to 0.51. The tetrahedral Al and interlayered K amount in ideal muscovite is 1, and the octahedral Al

amount is known as 2. The tetrahedral and octahedral substitutions and interlayer Ca and Na amounts in illites (0.05-0.12) make us consider that they are related with the expandable layer (smectite) component, the presence of other mica phases in clay fraction and most significantly with the diagenetic nature.

The major element compositions and structural formulae of illite and mixed-layered clay minerals (illite-chlorite I-C and chlorite-vermiculite C-V) by EDS method were given tables 3, 4 and 5; and the results were assessed with the ones performed by ICP method. The structural formulae of I-C and C-V mixed-layered clay minerals were estimated based on 12.5 atom (Weaver and Pollard, 1973).

Illites are located between montmorillonite and muscovite in the ternary diagram of tetrahedral substitution-octahedral substitution, but mostly in illite region (Figure 13a). Illites are located in montmorillonite − I-S − seladonite − phlogopite − muscovite pentagram in $M^{+}-4Si-R2^{+}$ diagram, but mostly between illite and muscovite (Figure 13b).

Illites are closer to Al^{IV} corner and have a composition between muscovite – phlogopite in the $Fe+Mg-Al^{IV}-Al^{VI}$ ternary diagram (Figure 14a). According to binary variation diagram of Na-K; Na low, but K presents a wide compositional interval (Figure 14b). However; they are aligned along muscovite-seladonite line, but close to muscovite corner in the Si-Al_{total} diagram (Figure 14c).

Illites are clustered in region parallel to the muscovite-seladonite line and closer to illite in the binary variation diagram of Si–(Na+K) (Figure 15a). However; in the Mg-Fe diagram they were aligned as parallel to the diagonal line of the rectangle showing a weak positive correlation (Figure 15b).

Illites were clustered close to muscovite corner in the binary variation diagram of Mg+Fe–Si in such a way that it shows a positive correlation though weak (Figure 16a). Interlayer cations possess a composition among muscovite-illite-phengite close to muscovite corner in Si/Al_{total} (Figure 16b).

The structural formulae of illite and mixed-layer clay minerals estimated starting from chemical analyses were given below:

Table 2- Major element chemical composition and structural formulas of illite minerals (ΣFeO: total iron, LOI: Loss on Ignition, TC: Tetrahedral charge, TOC: Total octahedral cation, OC: Octahedral charge, ILC: Interlayer charge, TLC: Total layer charge).

Oxide %	BZB-8	BZB-89	BZB-131	Mean
SiO_2	60.11	54.69	50.31	55.04
TiO_2	0.848	0.893	0.834	0.86
Al_2O_3	18.48	19.53	24.31	20.77
ΣFe_2O_3	5.70	7.13	4.88	5.90
MnO	0.010	0.019	0.011	0.01
MgO	1.45	1.95	1.86	1.75
CaO	0.72	0.88	0.34	0.65
Na_2O	0.12	0.37	0.18	0.22
K_2O	4.38	4.17	5.70	4.75
P_2O_5	0.21	0.22	0.20	0.21
LOI	7.43	8.59	10.06	8.69
Total	99.46	98.44	98.67	98.86
Si	3.96	3.75	3.51	3.74
Al	0.04	0.25	0.49	0.26
TC	0.04	0.25	0.49	0.26
Al	1.40	1.33	1.51	1.41
Ti	0.04	0.05	0.04	0.04
Fe	0.28	0.37	0.26	0.30
Mn		0.01		0.00
Mg	0.14	0.20	0.19	0.18
TOC	1.86	1.96	1.98	1.93
OC	0.52	0.38	0.15	0.35
Ca	0.05	0.07	0.03	0.05
Na	0.02	0.05	0.02	0.03
K	0.37	0.36	0.51	0.41
P	0.01	0.01	0.01	0.01
ILC	0.54	0.60	0.65	0.59
TLC	0.56	0.63	0.64	0.61

$(Ca_{0.05}Na_{0.03}K_{0.41}P_{0.01})(Al_{1.41}Ti_{0.04}Fe_{0.30}Mg_{0.18})[(Si_{3.74}Al_{0.26})O_{10}](OH)_2$ (Illite-ICP)

$(Mg_{0.02}Ca_{0.01}Na_{0.08}K_{0.77})(Al_{1.76}Ti_{0.02}Fe_{0.14}Mg_{0.12})[(Si_{3.23}Al_{0.77})O_{10}](OH)_2$ (Illite-EDS)

$(Mg_{0.23}Ca_{0.12}K_{0.07})(Al_{1.69}Fe_{1.05}Mg_{0.90})[(Si_{3.75}Al_{0.25})O_{10}](OH)_6$ (C-V-EDS)

$(Mg_{0.01}Ca_{0.12}K_{0.47})(Al_{1.90}Fe_{0.85}Mg_{0.80})[(Si_{3.28}Al_{0.72})O_{10}](OH)_6$ (I-C-EDS)

6.2. Trace Element Geochemistry

The trace element contents of illite minerals by ICP-MS method were presented in table 6. When distribution of trace elements with respect to their content is taken in 1 ppm reference interval; there is observed 385 times increase (Ba) and 100 times decrease (Bi and In). Looking at REE contents; 72 times increase (Ce) and

Table 3- EDS results (%) and structural formulas of illite minerals from the Kayabaşı formation (TC: Tetrahedral charge, TOC: Total octahedral cation, OC: Octahedral charge, ILC: Interlayer charge, TLC: Total layer charge).

Sample No.	BZB-17	BZB-45			BZB-71							
Mineral No.	m1	m1	m2	m3	m1			m2			m3	
Spectrum No.	s3	s8	s2	s1	s1	s2	s6	s2	s3	s9	s2	s10
SiO_2	50.234	50.784	48.890	50.567	48.075	50.895	50.049	48.482	47.145	49.498	47.620	50.420
TiO_2	0.685		0.593	0.361			0.613	0.642	0.368	0.450	0.400	
Al_2O_3	34.668	38.489	37.956	38.014	37.200	33.281	35.182	35.539	35.029	35.970	38.290	35.818
FeO	2.522	1.750	1.555	1.426	1.725	2.619	2.456	2.953	5.874	1.868	1.564	2.040
MnO												
MgO	1.5681	0.921	0.701	0.828	1.0989	2.282	1.507	1.409	2.4557	1.425	0.855	1.327
CaO		0.439					0.437		0.676	0.388		1.104
Na_2O	0.5530	0.639	0.560	0.708	0.895		0.644	1.112	0.656	0.984	1.213	0.728
K_2O	9.772	6.980	9.747	8.087	10.335	10.925	9.114	9.660	7.868	9.420	10.055	8.554
Total	100.00	100.00	100.00	99.99	99.33	100.00	100.00	99.80	100.07	100.00	100.00	99.99
Tetrahedral												
Si	3.18	3.14	3.08	3.14	3.07	3.23	3.16	3.09	3.02	3.12	3.02	3.17
Al	0.82	0.86	0.92	0.86	0.93	0.77	0.84	0.91	0.98	0.88	0.98	0.83
TC	0.82	0.86	0.92	0.86	0.93	0.77	0.84	0.91	0.98	0.88	0.98	0.83
Octahedral												
Al	1.76	1.94	1.89	1.92	1.87	1.72	1.77	1.76	1.67	1.80	1.88	1.82
Ti	0.03	0.00	0.03	0.02			0.03	0.03	0.02	0.02	0.02	
Fe^{2+}	0.13	0.09	0.08	0.07	0.09	0.14	0.13	0.16	0.31	0.10	0.08	0.11
Mn												
Mg	0.15		0.02	0.01	0.10	0.22	0.14	0.13	0.14	0.13	0.06	0.12
OC	0.04	0.00	0.01	0.00	0.01	0.12	0.03	0.02	0.01	0.06	0.00	0.08
TOC	2.07	2.01	2.02	2.02	2.06	2.08	2.07	2.08	2.14	2.05	2.04	2.05
Interlayer												
Mg		0.09	0.05	0.07					0.09		0.02	
Ca		0.03					0.03		0.05	0.03		0.07
Na	0.07	0.08	0.07	0.09	0.11		0.08	0.14	0.08	0.12	0.15	0.09
K	0.79	0.55	0.78	0.64	0.84	0.89	0.73	0.79	0.64	0.76	0.81	0.69
ILC	0.86	0.87	0.95	0.87	0.95	0.89	0.87	0.93	1.00	0.94	1.00	0.92
TLC	0.86	0.86	0.93	0.86	0.94	0.89	0.87	0.93	0.99	0.94	0.98	0.91
Sample No.	BZB-62											
Mineral No.	m1	m4	m4	m6	m6	m6	m6	m6	m6	m7	m9	
Spectrum No.	s3	s10	s12	s2	s3	s5	s6	s7	s9	s6	s3	
SiO_2	50.574	48.874	49.224	53.620	49.140	49.512	48.928	53.053	50.318	48.614	49.896	
TiO_2		0.352	0.445		0.661					0.658		
Al_2O_3	35.221	37.528	35.092	33.769	36.350	36.228	39.355	32.615	36.217	37.722	36.690	
ΣFeO	2.133	1.662	2.287	2.089	1.710	2.285	1.104	2.897	1.773	1.514	1.692	
MnO												
MgO	1.4382	0.861	1.364	2.497	1.4369	1.294	0.734	1.102	1.3107	1.110	1.3159	
CaO			1.202	0.760		0.748	0.801	0.476				
Na_2O	0.8706	1.092			0.4665	0.529	1.371	0.806	1.273	1.210	0.8347	
K_2O	9.765	9.633	10.389	7.265	10.237	9.406	7.710	9.052	9.070	9.174	9.570	
Total	100.00	100.000	100.00	100.00	100.00	100.00	100.00	100.00	99.96	100.00	100.00	
Tetrahedral												
Si	3.19	3.08	3.13	3.32	3.11	3.13	3.05	3.34	3.16	3.06	3.14	
Al	0.81	0.92	0.87	0.68	0.89	0.87	0.95	0.66	0.84	0.94	0.86	
TC	0.81	0.92	0.87	0.68	0.89	0.87	0.95	0.66	0.84	0.94	0.86	
Octahedral												
Al	1.81	1.87	1.76	1.78	1.82	1.83	1.94	1.76	1.84	1.86	1.86	
Ti		0.02	0.02		0.03					0.03		
Fe^{2+}	0.11	0.09	0.13	0.11	0.09	0.12	0.06	0.15	0.09	0.08	0.09	
Mn												
Mg	0.14	0.06	0.13	0.22	0.13	0.12	0.03	0.10	0.12	0.07	0.12	
OC	0.07	0.01	0.12	0.00	0.00	0.03	0.00	0.22	0.06	0.00	0.01	
TOC	2.06	2.04	2.04	2.11	2.07	2.07	2.03	2.01	2.05	2.04	2.07	
Interlayer												
Mg		0.02	0.01	0.01	0.01		0.04			0.03		
Ca			0.08	0.05		0.05	0.05	0.03				
Na	0.11	0.13			0.06	0.07	0.17	0.10	0.16	0.15	0.10	
K	0.79	0.78	0.84	0.57	0.83	0.76	0.61	0.73	0.73	0.74	0.77	
ILC	0.90	0.95	1.00	0.69	0.91	0.88	0.96	0.89	0.89	0.95	0.87	
TLC	0.88	0.93	0.99	0.68	0.89	0.90	0.95	0.89	0.90	0.94	0.86	

Table 4- EDS results (%) and structural formulas of illite minerals of the Mahmut Tepesi formation (TC: Tetrahedral charge, TOC: Total octahedral cation, OC: Octahedral charge, ILC: Interlayer charge, TLC: Total layer charge).

Sample No.	BZB-178									
Mineral No.	m3			m2	m8		m1			m2
Spectrum No.	s4	s6	s8	s3	s9	s12	s3	s5	s8	s4
SiO_2	62.490	56.650	60.410	59.544	57.676	58.292	52.140	51.760	51.074	50.347
TiO_2		0.330		1.610		0.409			0.389	
Al_2O_3	22.230	23.500	25.430	20.258	22.191	20.591	27.649	31.404	29.538	32.947
FeO	2.010	6.430	1.550	4.590	6.668	7.205	3.801	2.269	4.580	3.064
MnO										
MgO				2.643	3.417	3.495	3.689	2.584	2.847	2.654
CaO			0.330							
Na_2O					0.473			1.045		0.511
K_2O	12.370	10.690	10.840	11.355	9.574	10.007	11.779	10.485	11.572	10.476
Total	99.10	97.60	98.56	100.00	100.00	100.00	99.06	99.55	100.00	100.00
Tetrahedral										
Si	3.95	3.72	3.81	3.80	3.69	3.74	3.39	3.30	3.30	3.21
Al	0.05	0.28	0.19	0.20	0.31	0.26	0.61	0.70	0.70	0.79
TC	0.05	0.28	0.19	0.20	0.31	0.26	0.61	0.70	0.70	0.79
Octahedral										
Al	1.61	1.54	1.70	1.32	1.37	1.31	1.50	1.66	1.54	1.68
Ti		0.02		0.08		0.02			0.02	
Fe^{2+}	0.11	0.35	0.08	0.25	0.36	0.39	0.21	0.12	0.25	0.16
Mn										
Mg				0.25	0.33	0.34	0.36	0.25	0.27	0.25
OC	0.95	0.60	0.74	0.72	0.51	0.57	0.34	0.28	0.26	0.14
TOC	1.72	1.91	1.78	1.90	2.06	2.06	2.07	2.03	2.08	2.09
Interlayer										
Mg										
Ca			0.02							
Na					0.06			0.13		0.06
K	1.00	0.90	0.87	0.93	0.78	0.82	0.98	0.85	0.95	0.85
ILC	1.00	0.90	0.91	0.93	0.80	0.82	0.98	0.98	0.95	0.91
TLC	1.00	0.88	0.93	0.92	0.82	0.83	0.95	0.98	0.96	0.93

3 times decrease (Lu) is observed. Besides; the tracing of REE contents from La to Lu in the form of increase-decrease indicate the consistency of analyses and that illites are pure or nearly pure.

The chondrite-normalized distribution of trace element contents of illites (Sun and McDonough, 1989) was given in figure 17. The Nb and Y from Condie (1993) and the other elements were taken from Gromet et al. (1984) for NASC. When compared with chondrite values; the enrichment (579 times for U) - depletion (4 times for P) in elements based on the host-rock it derived vary and pattern minerals distinguish from NASC and each other. In other word; the illites exhibit distinctive differentiation / fractionation. The most distinctive positive and negative anomalies are recorded in La, Nd and Ti; and Sr and P elements, respectively.

The REE contents of illite minerals were normalized according to chondrite (Sun and McDonough, 1989) and their element abundances were compared (Figure 18). The values of the North American Shales (North American Shale Composite, NASC) were also added to the diagram (for Ho and Tm elements; Haskin et al., 1968, for other elements; Gromet et al., 1984).

According to chondrite values, illite minerals and NASC patterns resemble to each other, however; they differentiation from each other in term of abundances and show distinctive differentiation / fractionation. The REE contents of illites, except the La-Ce-Pr, are lower than NASC but increased with respect to chondrite (174 times for La, 10 times for Ho). Besides; LREE concentrations of illite minerals show a decrease with respect to HREE. There is also observed a small decrease for Eu.

Table 5- EDS results (%) and structural formulas of chlorite interlayered minerals in rocks of the Bozkır Unit (TC: Tetrahedral charge, TOC: Total octahedral cation, OC: Octahedral charge, ILC: Interlayer charge, TLC: Total layer charge).

Mineral	C-V	C-V	I-C
Sample No	BZB-45	BZB-71	BZB-178
Mineral No	1	3	2
Spectrum No	s6	s4	s6
SiO_2	42.926	43.440	43.470
TiO_2			
Al_2O_3	25.978	29.399	29.433
FeO	17.435	15.920	13.529
MnO			
MgO	11.959	8.390	7.189
CaO	1.303	1.726	1.452
Na_2O			
K_2O	0.402	1.123	4.925
Total	100.00	100.00	100.00
Tetrahedral			
Si	3.24	3.25	3.28
Al	0.76	0.75	0.72
TC	0.76	0.75	0.72
Octahedral			
Al	1.55	1.84	1.90
Ti			
Fe	1.10	1.00	0.85
Mn			
Mg	1.07	0.74	0.80
OC	0.01	0.00	0.00
TOC	3.72	3.58	3.55
Interlayer			
Mg	0.27	0.20	0.01
Ca	0.11	0.14	0.12
Na			
K	0.04	0.11	0.47
ILC	0.80	0.79	0.73
TLC	0.77	0.75	0.72

6.3. Stable Isotope Geochemistry

These analyses, which represent the oxygen and hydrogen isotope geochemistry of illites, are generally applied in two sections in order to determine the traces of geothermometer and fluid-rock interaction. The first is based on the differentiation between the two phases related to the formation temperatures, and the second is based on isotopic composition of fluid or rock in order to assess the origin of fluid or rock protoliths. In other words; if the origin of the water is known (sea water, meteoric, magmatic) then temperature conditions; if temperature conditions are known then the origin of water is detected. Oxygen and hydrogen isotope geochemistry analyses were carried out on 3 illite minerals (Table 7).

In addition to $\delta^{18}O$ and δD values of illite minerals, the sea water point, meteoric water and supergene-hypogene lines, which had been suggested by many investigators (Craig, 1961; Sheppard et al., 1969; Sheppard, 1986; Sheppard and Gilg, 1996; Wenner and Taylor, 1974), were also added to figure 19. In $\delta^{18}O$ – δD diagram according to isotopic change of water vs. increasing temperature, the isotopic composition of the water, which constitute I-S, is far from the sea water composition but is located between East Mediterranean Meteoric Water (EMMW, Gat et al., 1996) composition and the magmatic water composition. In the determination of illite-water equilibrium, which changes with temperature, R3 for oxygen; Savin and Lee (1988) equation for I-S (90 % I, 10 % S) and Yeh (1980) equation for hydrogen were used. It is considered that diagenetic waters forming

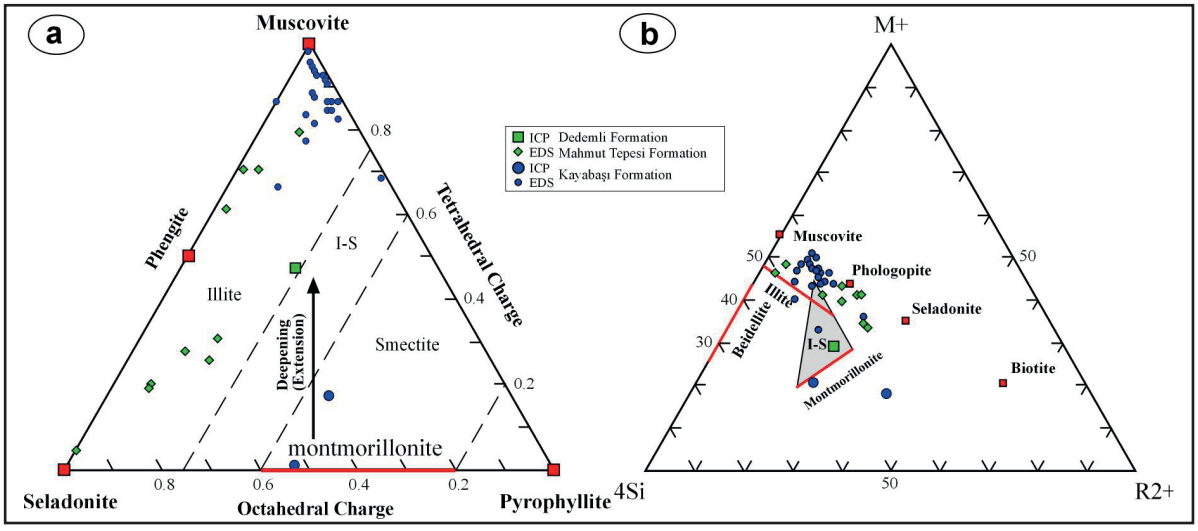

Figure 13- The distributions of cations from clay minerals in the triangular diagrams, a) Tetrahedral charge-octahedral charge, b) M^{+}-4Si-R^{2+}.

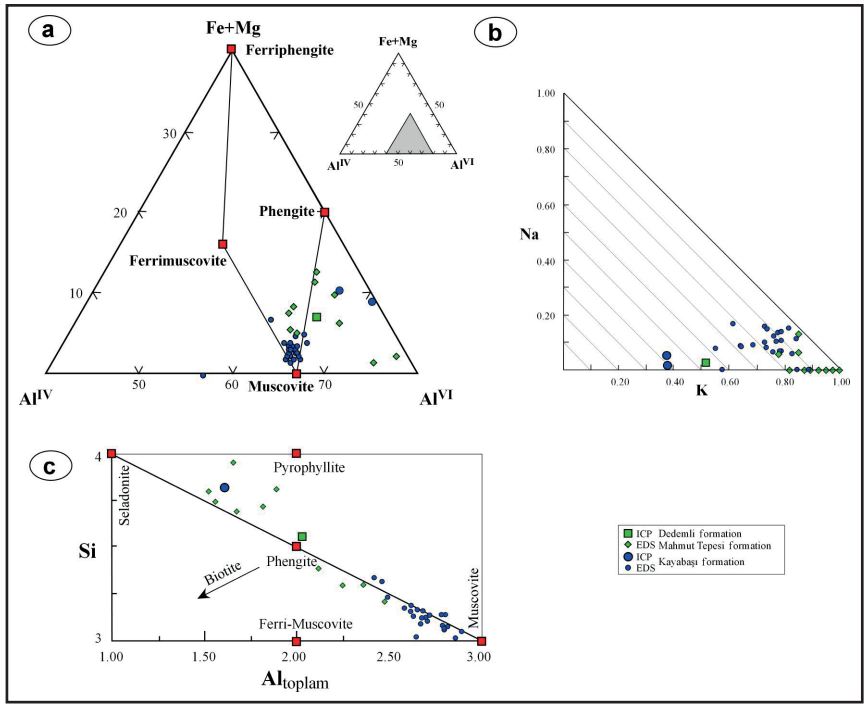

Figure 14- The distributions of cations from clay minerals in the triangular and binary diagrams, a) octahedral (Fe+Mg)-octahedral Al^{VI}-tetrahedral Al^{IV}, b) Interlayers Na-K, c) Tetrahedral Si-Al_{total}.

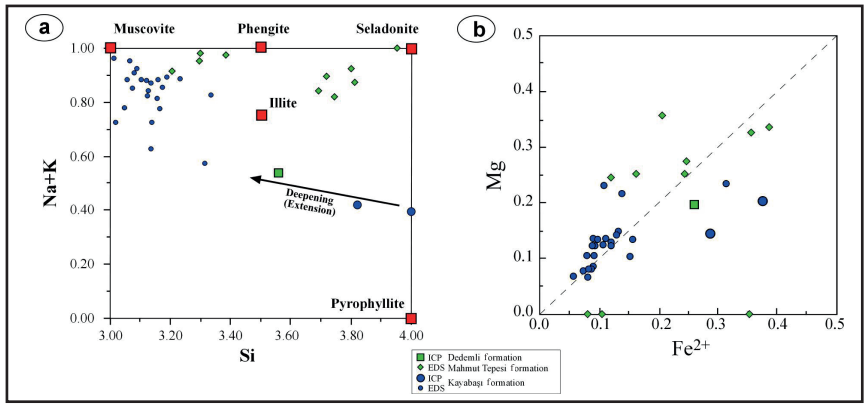

Figure 15- The distributions of cations from clay minerals in the variation diagrams, a) Interlayer Na+K-tetrahedral Si, b) Octahedral Mg-Fe.

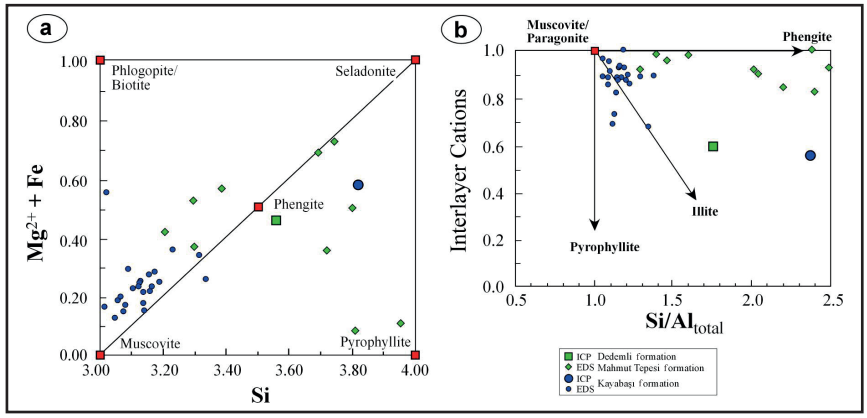

Figure 16- The distributions of cations from clay minerals in the variation diagrams, a) Octahedral Mg+Fe-tetrahedral Si, b) tetrahedral Si/Al_{total}.

Table 6- Trace element chemical compositions of illite minerals.

Element (ppm)	BZB-8	BZB-89	BZB-131	Mean
Cr	120	150	180	150
Ni	40	60	90	63
Co	6	9	13	9
Sc	14	16	17	16
V	160	187	224	190
Cu	30	30	40	33
Pb	15	11	15	14
Zn	150	310	130	197
Bi	0.1	0.3	<0.1	0.2
In	<0.1	<0.1	<0.1	0.1
Sn	4	5	6	5
W	2.7	5.7	2.1	3.5
Mo	<2	<2	<2	2
As	85	17	16	39
Sb	0.8	0.4	<0.2	0.5
Ge	2.0	2.6	2.8	2.5
Be	3	3	3	3
Ag	1.8	1.4	1.3	1.5
Rb	163	201	254	206
Cs	34.1	17.5	49.8	33.8
Ba	258	385	322	322
Sr	107	120	196	141
Tl	0.91	0.91	1.19	1.00
Ga	24	29	36	30
Ta	1.34	1.42	1.39	1.38
Nb	18.0	19.4	18.4	18.6
Hf	4.1	4.0	3.5	3.9
Zr	164	165	140	156
Y	13.2	16.5	16.8	15.5
Th	11.6	13.1	16.7	13.8
U	4.04	3.56	4.63	4.08
La	30.00	35.00	41.30	35.43
Ce	52.3	63.5	72.0	62.6
Pr	6.04	7.56	8.61	7.40
Nd	20.5	26.3	29.5	25.4
Sm	3.48	4.21	4.47	4.05
Eu	0.667	0.815	0.826	0.769
Gd	2.50	3.25	3.05	2.93
Tb	0.43	0.52	0.51	0.49
Dy	2.62	3.18	3.11	2.97
Ho	0.55	0.68	0.67	0.63
Er	1.67	2.04	2.08	1.93
Tm	0.279	0.322	0.352	0.318
Yb	1.91	2.25	2.37	2.18
Lu	0.301	0.342	0.342	0.328

Table 7- Stable isotope compositions ($\delta^{18}O$ ve δD) of illite minerals.

Sample No	Yield %	% H_2O	dD(SMOW)	$d^{18}O$(SMOW)
BZB-8	14.8	8.6	-72	20,8
BZB-89	14.1	10.7	-75	18.3
BZB-131	14.2	12.1	-71	19.7

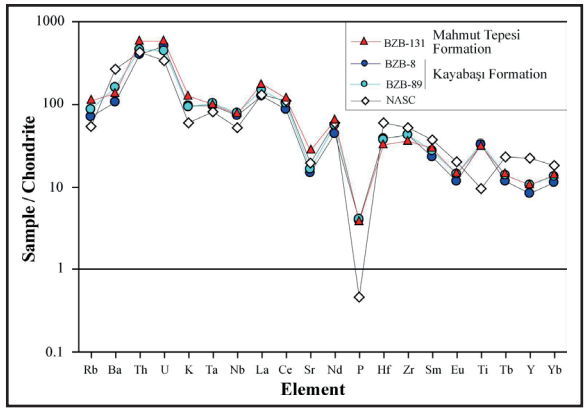

Figure 17- Chondrite-normalized trace element patterns of the illite minerals (Chondrite: Sun and McDonough, 1989; Nb and Y for NASC: Condie, 1993; other elements: Gromet et al., 1984).

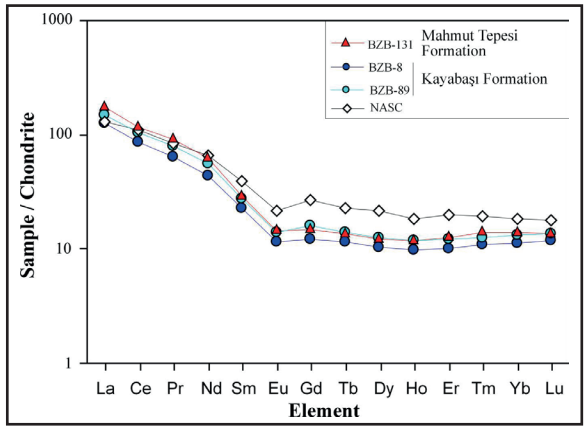

Figure 18- Chondrite-normalized REE abundances of the illite minerals (NASC: Ho and Tm elements from Haskin et al., 1968, other elements: Gromet et al., 1984; Chondrite: Sun and McDonough, 1989).

the illites which are closely located to the EMMW composition are mostly originated from groundwater and partly from volcanic-volcano-sedimentary waters.

According to $\delta_{18}O_{H2O}$ – temperature (°C) diagram, when the water forming the illites are completely assumed as EMMW then temperature conditions lower than 20 °C; and when it is assumed to be the magmatic water then temperature conditions higher than 80 °C were obtained (Figure 20). The crystal-chemical data (KI, crystallite size, d_{060}, polytype, etc.) of illites foresees temperature conditions higher than 20 °C and seems to be related with the mixture of two different waters. The isotope data of illites in sample BZB-8 representing the section away from the rifting of the Kayabaşı Formation and the illites in sample BZB-89 representing the section close to rifting indicate a temperature difference reaching 10 °C for

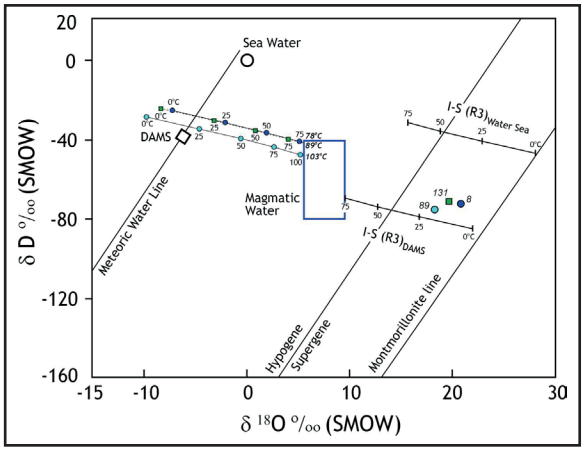

Figure 19- The setting of oxygen and hydrogen isotope compositions of the illite minerals in the $\delta^{18}O$ and δD diagram (Supergene-hypogene line: Sheppard et al., 1969; meteoric water line: Craig, 1961).

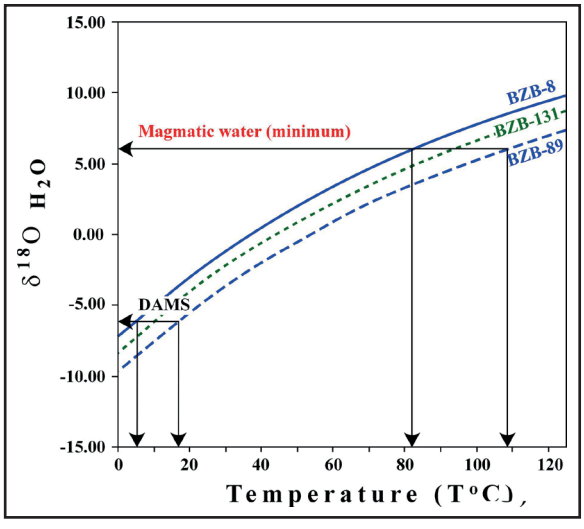

Figure 20- Relationships between ‰ $\delta^{18}O$ (SMOW) values and temperature of water forming illites (DAMS from Gat et al., 1996; magmatic water composition from Taylor, 1968).

the groundwater origin and 30 °C for the magmatic water origin. This situation makes us consider that the temperature increase of which the rifting had caused affected the illite isotope chemistry.

7. Discussion and Results

The results obtained from volcanic, pyroclastic, epiclastic and carbonate rocks of the Bozkır Unit between Triassic-Cretaceous intervals are mostly related with rifting, crustal thinning and partly with burial diagenesis and were mentioned below (Figure 21).

Illites are different in origin in diagenetic sediments (detritic / residual, authigenic) but there occurs ordering in their crystal structure by means of burial effects. With increasing diagenesis, the crystallographic parameters of illite can be used as the grading scale (especially KI). In addition to increasing heat flow related with rifting from diagenesis to metamorphism, there is observed a decrease in KI values (peak narrowing), and $1M_d$ and $1M$ polymorphic types are replaced by $2M_1$. Fine grained micas named as sericite as textural take the place of illites (Duyoner de Segonzac, 1970). The K_2O amount and total negative interlayer capacity of the illites increase in the direction of diagenesis → anchizone → epizone with increasing diagenetic / metamorphic grade (Hunkizer et al., 1986; Bozkaya and Yalçın, 1999).

According to OM and SEM analyses, illite/mica minerals encountered in the Bozkır Unit rocks are widely represented by diagenetic illite, few detritic and volcanogenic micas.

In addition to volcanic glass and/or matrix, typical in volcanogenic rocks, it is considered by many investigators (Yalçın and Gümüşer, 2000; Yalçın and Bozkaya, 2003; Yalçın et al., 2005), who studied in similar environments, that the cations, which occur by the decomposition of K-feldspars with sea water and not used in other phyllosilicate structure, caused the formation illite/muscovites:

(Volcanic glass and/or matrix → Aqueous Al- or Kal siicate gel → Illite/muscovite)

$$3SiO_2.2Al_2O_3+12H_2O \rightarrow 2Al_2(OH)_6.3Si(OH)_4+K^+ \rightarrow KAl_3(Si_3AlO_{10})(OH)_2+10H_2O+2OH^-$$

$$6SiO_2.3Al_2O_3.K_2O+21H_2O \rightarrow K_2O.6Al(OH)_3.6Si(OH)_4 \rightarrow 2KAl_2[AlSi_3O_{10}](OH)_2+19H_2O$$

(K-feldspar or feldspar → Illite/Muscovite and/or Quartz)

$$3(Na,K,Ca)Al_2Si_2O_8+4H^++2K^+ \rightarrow 2KAl_2[AlSi_3O_{10}](OH)_2+3(Na^+,K^+,Ca^{2+})$$

$$4KAlSi_3O_8+6H^+ \rightarrow KAl_3(Si_3AlO_{10})(OH)_2+9SiO_2+2H_2O+3K^+$$

In all geological times, the chlorites in sedimentary rocks are observed as residual in degradation profiles starting from the regressive metamorphism or diagenesis of the host-rock. However, they were

derived either from the alteration zones or completely from the alteration of green schists in which the whole component is chlorite in sedimentary basins. The chlorites are formed from irregular three layered clay minerals as a result of aggradation in marine environments. In the early diagenesis, irregular chlorites are subjected to aggradation because of Mg rich interstitial solutions. As the chlorites that occurred in the early diagenesis are generally rich in Fe, while the Mg content increases with increasing depth by the increasing diagenesis-metamorphism (Ahn and Peacor, 1985).

The chlorites in volcanic, pyroclastic and epiclastic rocks representing the rocks of the Bozkır Unit occur in bonding material and pores. OM and SEM analyses show that the chlorite developed authigenically in pores rather than dark-colored minerals. However; in volcanogenic rocks, it can be stated that the volcanic glass-chlorite transformation occurred passing through an aqueous MgFeAl-silicate gel interphase (e.g. Çerikçioğlu and Yalçın, 1998; Yalçın and Bozkaya, 2002; Yalçın et al., 2005):

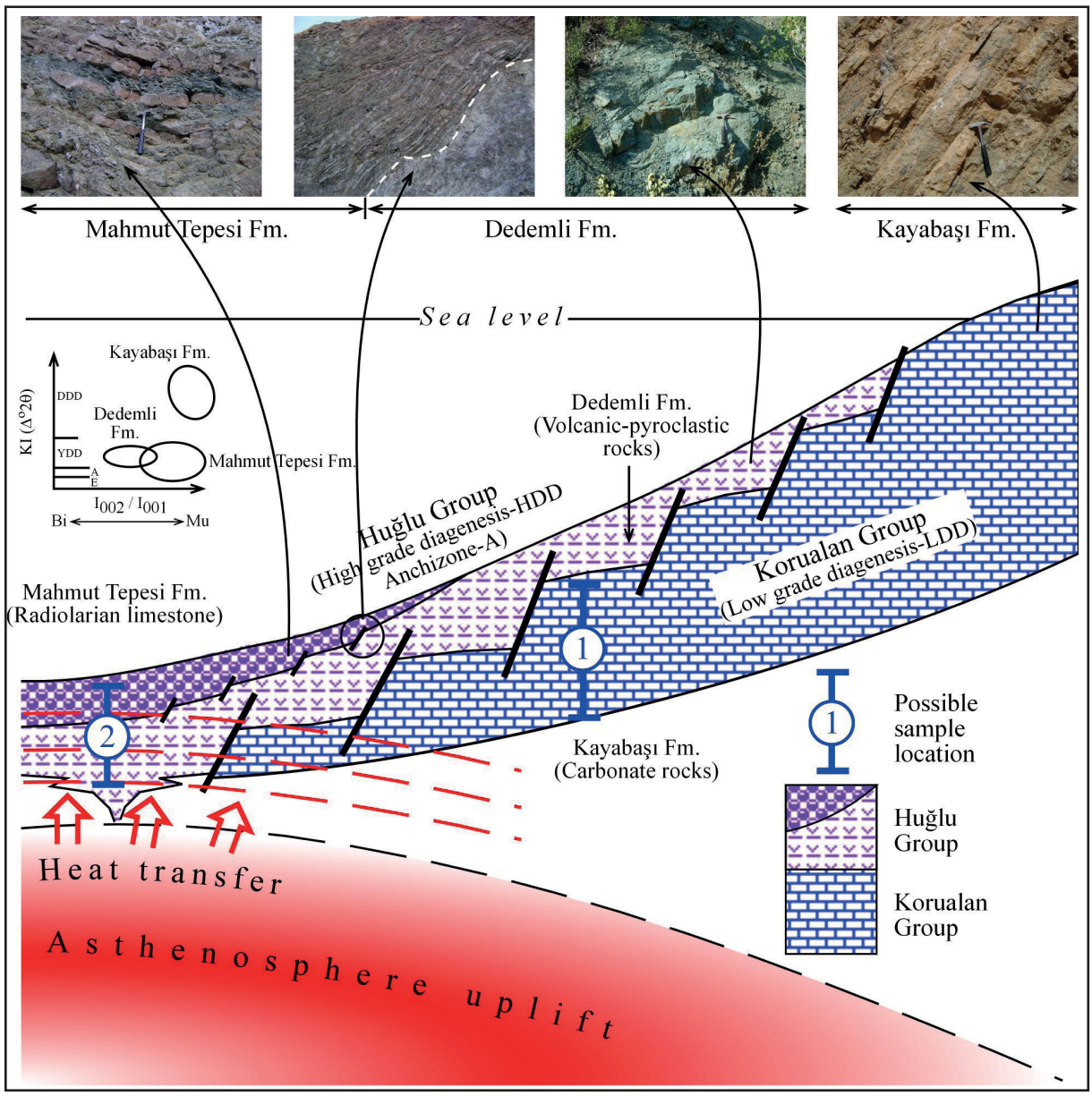

Figure 21- Schematic display of the thermal maturation (diagenesis / metamorpism grade) differrences related to rifting of Bozkır Unit rocks.

(Matrix and/or volcanic glass → Aqueous MgFeAl-silicate gel → Chlorite)

$7SiO_2.Al_2O_3.2MgO.2FeO+24OH^-+10H^+ \rightarrow 9MgO.2FeO.2Al(OH)_3.7Si(OH)_4 \rightarrow Mg_9Fe_2Al[AlSi_7O_{20}](OH)_{16}+9H_2O$

The diagenesis can only be possible by one interlayered phase stage (aggradation) such as the occurrence of these minerals, which have a special significance in studies related with very low grade metamorphism or by the transformation of smectite into illite or chlorite. Non-expanding layer components (illite or chlorite) of the mixed clay layers to increase towards deeper parts or expanding layer components (smectite) to decrease and the order of stacking give important clues on advanced diagenesis (Frey, 1987; Merriman and Peacor, 1999).

The mixed-layered clay minerals widely observed during the late diagenesis are C-S, C-V, I-C and I-S. Mixed-layered C-V is a stage in the aggradation of the 2:1 layered vermiculite type which shows evolution towards chlorite (Dunoyer de Segonzac, 1970; Hoffman and Hower, 1979). Mixed layers I-S and I-C show an evolution towards illite or chlorite by the participation of K or Mg and/or Fe. The permeability is also important for the mobility of solutions in the transformation of smectite into illite or chlorite and to play an active role.

The transformation of smectite into chlorite mostly occurs starting from regular interlayered stage, and 1:1 ordered C-S or C-V mixed layers called as corrensite is formed. Corrensite is widespread in basic and intermediate pyroclastic and volcanoclastic rocks (Evarts and Schiffman, 1983; Brigatti and Poppi, 1984; Inoue et al., 1984, 1987; Inoue, 1985, 1987; Bettison and Schiffman, 1988; Inoue and Utada, 1991), especially in the laumontite zone of the zeolite zone (Kübler et al., 1974; Boles and Coombs, 1977; Lippmann and Rothfuss, 1980; Kisch, 1980, 1981). These minerals are located at the contact metamorphism zones of shales (Blatter et al., 1973; April, 1980; Vergo and April, 1982) and besides in formations related with the burial diagenesis of octahedral clay minerals (Hoffman and Hower, 1979; Chang et al., 1986).

It is probable that the rocks, in which the mixed-layered clay minerals in siliciclastic and volcanic-volcanosedimentary units were derived, formed by the neoformation and/or transformation rather than detrital as being related with the origin material (e.g. Çerikçioğlu and Yalçın, 1998; Yalçın and Gümüşer, 2000; Yalçın and Bozkaya, 2002, 2003; Yalçın et al., 2005):

(Volcanic glass and/or matrix → Aqueous MgFeAl-silicate gel → C-S)

$7SiO_2.Al_2O_3.7MgO.FeO+11H_2O+12H^+ \rightarrow 7MgO.FeO.2Al(OH)_3.7Si(OH)_4 \rightarrow Mg_7FeAl[AlSi_7O_{20}](OH)_{12}+4H_2O+14H^+$

(Phlogopite-Biotite → I-V → Vermiculite)

$K(Mg,Fe)_3[AlSi_3O_{10}](OH)_2+0.50Ca^{+2}+4H_2O \rightarrow K_{0.5}Ca_{0.25}(Mg,Fe)_{3.0}[AlSi_3O_{10}](OH)_2.2H_2O$

$\rightarrow Ca_{0.5}(Fe,Mg)_3[AlSi_3O_{10}](OH)_2.4H_2O+K^+$

(Volcanic glass → Aqueous NaKAl-silicate gel → I-S)

$6SiO_2.3Al_2O_3.Na_2O.K_2O+19H_2O+4H^+ \rightarrow Na_2O.K_2O.6Al(OH)_3.6Si(OH)_4 \rightarrow KNaAl_4[Al_2Si_6O_{20}](OH)_4+18OH^-$

(Sanidine/Orthoclase or plagioclase → I-S)

$6KAlSi_3O_8+Na^++4H_2O \rightarrow KNaAl_4[Al_2Si_6O_{20}](OH)_4+12SiO_2+5K^++4OH^-$

$3(Na,Ca)Al_2Si_2O_8+2H_2O+K^++2H^+ \rightarrow KNaAl_4[Al_2Si_6O_{20}](OH)_4+2(Na^+,Ca^{2+})+2OH^-$

(Volcanic glass and/or matrix → Aqueous KMgFeAl-silicate gel → I-C)

$7SiO_2.4Al_2O_3.2FeO.9MgO.K_2O+25H_2O+2OH^- \rightarrow K_2O.9MgO.2FeO.8Al(OH)_3.7Si(OH)_4$

$\rightarrow K_2Mg_9Fe_2Al_5[Al_3Si_7O_{40}](OH)_{20}+4H_2O+24H^+$

According to KI and AI ($\Delta°2\theta$) data; The Kayabaşı formation has low grade diagenesis, the Dedemli formation has high grade formation and the Mahmut Tepesi formation has high grade digenesis and anchizone degree. With increasing degree of diagenesis the smectite component of illites decreases. The illite/micas of the Kayabaşı formation are muscovitic and the illite/micas of the Mahmut Tepesi formation related to rifting are phenitic and seladonitic in composition among pre-rift units. The chondrite based distribution of trace and REEs contents in illites present a similar orientation for the Kayabaşı and Dedemli formations, but the amounts of these elements increase few in the Dedemli formation.

According to $\delta^{18}O$–δD isotopic change of illite minerals with increasing temperature, the isotopic composition of the water which forms these minerals are away from the sea water composition, but it is located between EMMW and the magmatic water compositions. This situation makes us consider that the diagenetic fluids forming illites mostly originated from the groundwater (diagenetic water or the formation water), and partly from magmatic water (volcanic-volcanosedimentary). According to $\delta^{18}O_{H2O}$-temperature relationship; when the water, forming the illite minerals, are completely assumed as the East Mediterranean Meteoric Water (EMMW) then low (<20 °C) temperature conditions; and when it is assumed as the magmatic water then high (>80 °C) temperature conditions are satisfied. Thus; these diagenetic conditions can be explained by the interaction (rock-water interaction) of meteoric waters with volcanic rocks. The isotope data show that the probable rifting effect caused a temperature difference reaching up to 30 °C in the formation illite, that is; the temperature increase also reflected to the isotope chemistry of illite.

In conclusion; clay and very few observed zeolite minerals in the Bozkır Unit was formed by the neoformation mechanism starting from fluids / solutions that occur as a result of decomposition of the volcanic material with sea water. The clay minerals in diagenesis and very low grade metamorphism conditions on the other hand; were re-ordered by the transformation mechanism with diagenetic solutions subjected to interaction with volcanogenic rocks. The textural, mineralogical and geochemical data of the Bozkır Unit rocks present significant differences based on the temperature increase related to rifting. It seems that the rifting has also affected the chemical compositions of minerals in addition to lithological differences and the degree of diagenesis / metamorphism.

Acknowledgements

This study was supported by the project numbered as M-477 by the Scientific Research Projects of the Cumhuriyet University. We would like to thank to technical staffs in the laboratories of the Geological Engineering Department for their helps during thin-section and XRD analyses, to Geol. Eng. Deniz Hozatlıoğlu (MS) for his contributions during field studies and to Prof. Fernando NIETO for his logistical and scientific supports in SEM-EDS analyses in the Laboratories of the Granada University in Spain within framework of Erasmus. Besides; we would like to express our gratitude to referees and editors for their invaluable scientific criticisms during the preparation of this paper.

References

Ahn, J., Peacor, D.R. 1985. Transmission electron microscopic study of diagenetic chlorite in Gulf Coast argillaceous sediments. *Clays and Clay Minerals*, 33, 228-236.

Alan, İ., Şahin, Ş., Keskin, H., Kop, A., Balcı, V., Böke, N., Bakırhan, B., Altun, İ., Esirtgen, T., Elibol, H., Arman, S., 2014. Orta Toroslar'da Hadim-Taşkent (Konya) yöresinde tektono-stratigrafik istiflerde yeni bulgular: Kartal Dağı istifi. *67. Türkiye Jeoloji Kurultayı*, 14-18 April 2014, 60-61.

Andrew, T., Robertson, A.F., 2002. The Beyşehir–Hoyran–Hadim Nappes: genesis and emplacement of Mesozoic marginal and oceanic units of the northern Neotethys in southern Turkey. *Journal of the Geological Society*, *London*, 159, 529–543.

April, R.H. 1980. Regularly interstratified chlorite/vermiculite in contact metamorphosed red beds, Newark Group, Connecticut Valley. *Clays and Clay Minerals*, 28, 1-11.

Arkai, P. 1991. Chlorite crystallinity: an empirical approach and correlation with illite crystallinity, coal rank and mineral facies as examplified by Palaeozoic and Mesozoic rocks of northeast Hungary. *Journal of Metamorphic Geology*, 9, 723-734.

Bailey, S.W. 1980. Structure of Layer Silicates. In: Crystal Structures of Clay Minerals and Their X-ray Identification, G.W. Brindley and G. Brown (Eds.), Mineralogical Society, London, 1-123.

Bailey, S.W. 1988. X-ray diffraction identification of the polytypes of mica, serpentine, and chlorite. *Clays and Clay Minerals*, 36, 193-213.

Bettison, L.A., Schiffman, P. 1988. Compositional and structural variations of phyllosilicates from the Point Sal ophiolite, California. *American Mineralogist*, 73, 62-76.

Blatter, C.L., Roberson, H.E., Thompson, G.R. 1973. Regularly interstratified chlorite-dioctahedral smectite in dike-intruded shales, Montana. *Clays and Clay Minerals*, 21, 207-212.

Blumenthal, M.M. 1944. Bozkır güneyinde Toros sıradağlarının serisi ve yapısı. İÜFF Mec., SeriB, 9, 95-125.

Blumenthal, M.M. 1947. Seydişehir-Beyşehir hinterlandındaki Toros Dağlarının jeolojisi. *Bulletin of Min. Res. And Exp.*, Seri D, 2, 242 p.

Blumenthal, M.M. 1951. Batı Toroslarda Alanya ard ülkesinde jeolojik araştırmalar. *Bulletin of Min. Res. And Exp.*, Seri D, 5, 194 p.

Blumenthal, M.M. 1956. Karaman Konya havzası güneybatısında Toros kenar silsilesi ve şist-radyolarit formasyonu stratigrafi meselesi. *Bulletin of Min. Res. And Exp.*, 48, 1-36.

Boles, J.R., Coombs, D.S. 1977. Zeolite facies alteration of sandstones in the Southland Syncline, New Zealand. *American Journal of Science*, 277, 982-1012.

Bozkaya, Ö., Yalçın, H. 1996. Diyajenez-metamorfizma geçişinin belirlenmesinde kullanılan yöntemler. *Jeoloji Mühendisliği Dergisi*, 49, 1-22.

Bozkaya, Ö., Yalçın, H. 1997*a*. Aygörmez Dağı napı (Pınarbaşı-Kayseri) Devoniyen-Triyas yaşlı diyajenetik-çok düşük dereceli meta-sedimanter kayaçların mineralojik ve petrografik özellikleri. Çukurova Üniversitesinde Jeoloji Mühendisliği Eğitiminin 20. Yılı Sempozyumu, *Geosound*, Special Edition, Vol. II, 30, 807-832.

Bozkaya, Ö., Yalçın, H. 1997*b*. Bolkardağı Birliği (Orta Toroslar, Bozkır-Konya) Üst Paleozoyik-Alt Mesozoyik yaşlı diyajenetik-çok düşük dereceli metamorfik kayaçların mineralojisi ve petrografisi. H.Ü. *Yerbilimleri*, Baysal Batman Special Issue, 19, 17-40.

Bozkaya, Ö., Yalçın, H. 1998. Doğu Toros Otoktonu Paleozoyik kayalarında gömülme ile ilişkili diyajenez ve çok düşük dereceli metamorfizma. Bulletin of Turkish Association of the Petroleum Geologists, 10, 35-54.

Bozkaya, Ö., Yalçın, H. 1999. Doğu Toros Otoktonunda diyajenez-metamorfizma derecesi ile fillosilikatların kimyası arasındaki ilişkiler. 9. Ulusal Kil Sempozyumu, İstanbul Üniversitesi, İstanbul, 15-18 Eylül, Abstracts, 21-30.

Bozkaya, Ö., Yalçın, H. 2000. Very low-grade metamorphism of Upper Paleozoic-Lower Mesozoic sedimentary rocks related to sedimentary burial and thrusting in Central Taurus Belt, Konya, Turkey. *International Geology Review*, 42, 353-367.

Bozkaya, Ö., Yalçın, H., Göncüoğlu, M.C. 2002. Mineralogic and organic responses to stratigraphic irregularities: an example from the Lower Paleozoic very low-grade metamorphic units of the Eastern Taurus Autochthon, Turkey. *Schweizerische Mineralogische und Petrographische Mitteilungen*, 82, 2, 355-373.

Bozkaya, Ö., Yalçın, H. 2004. New mineralogic data and implications for the tectono-metamorphic evolution of the Alanya Nappes, Central Tauride Belt, Turkey. *International Geology Review*, 46, 4, 347-365.

Bozkaya, Ö., Yalçın, H. 2005. Diagenesis and very low-grade metamorphism of the Antalya Unit: mineralogical evidence of Triassic rifting, Alanya-Gazipaşa, Central Taurus Belt, Turkey. Journal of Asian Earth Sciences, 25, 109-119.

Bozkaya, Ö., Yalçın, H. 2010. Geochemistry of mixed-layer illite-smectites from an extensional basin, Antalya Unit, Southwestern Turkey. *Clays and Clay Minerals*, 58, 644-666.

Bozkaya, Ö., Gürsu, S., Göncüoğlu, M.C. 2006*a*. Textural and mineralogical evidence for a Cadomian tectonothermal event in the eastern Mediterranean (Sandıklı-Afyon area, western Taurides, Turkey). *Gondwana Research*, 10, 301-315.

Bozkaya, Ö., Yalçın, H., Dündar, M.K. 2006*b*. Maden Grubu (Malatya-Pütürge) kayaçlarında diyajenez/metamorfizma ve jeotektonik konum arasındaki İlişkiler. C.Ü. *Mühendislik Fakültesi Dergisi Seri A-Yerbilimleri*, 23, 1-24.

Brigatti, M.F., Poppi, L. 1984. Crystal chemistry of corrensite: A review. *Clays and Clay Minerals*, 32, 391-399.

Brindley, G.W. 1980. Quantitative X-ray mineral analysis of clays. In: Crystal Structures of Clay Minerals and their X-ray Identification, G.W. Brindley and G. Brown (Eds.), Mineralogical Society, London, 411-438.

Brunn, J.H., Dumont, J.F., Graciansky, P.C., Gutnic, M., Juteau, T., Marcoux, J., Monod, O., Poisson, A. 1971. Outline of the Western Taurides. Geology and History of Turkey, Angus S. Compbelli (Ed.), Petroleum Exploration Society of Libya, Tripoli, 225-255.

Chang, H. K., Mackenzie, F. T., Schoonmaker, J. 1986. Comparisons between the diagenesis of dioctahedral and trioctahedral smectite, Brazilian offshore basins. *Clays and Clay Minerals*, 34, 407-423.

Clayton, R.N., Mayeda, T.K. 1963. The use of bromine pentafluoride in the extraction of oxygen from oxides and silicates for isotopic analysis. *Geochimica et Cosmochimica Acta*, 27, 43-52.

Condie, K.C. 1993. Chemical composition and evolution of the upper continental crust: Contrasting results from surface samples and shales. *Chemical Geology*, 104, 1-37.

Craig, H. 1961. Isotopic variations in meteoric waters. *Science*, 133, 1702-1703.

Çerikcioğlu, B., Yalçın, H. 1998. Yıldızeli-Akdağmadeni arasındaki (Yavu çevresi) Eosen yaşlı volkanojenik kayaçlarla ilişkili kil minerallerinin mineralojisi ve jeokimyası. C.Ü. *Mühendislik Fakültesi Dergisi Seri A-Yerbilimleri*, 15, 87-100.

Dunoyer de Segonzac, G. 1970. The transformation of clay minerals during diagenesis and low-grade metamorphism: A review. *Sedimentology*, 15, 281-346.

Eberl, D.D., Velde, B. 1989. Beyond the Kübler index. *Clay Minerals*, 24, 571-577.

Evarts, R.C., Schiffman, P. 1983. Submarine hydrothermal metamorphism of the Del Puerto Ophiolite, California. *American Journal of Science*, 283, 289-341.

Folk, R.L. 1974. Petrology of Sedimentary Rocks. Second edition, Hemphill Press, Austin, TX, 182 p.

Frey, M. 1987. Very low-grade metamorphism of clastic sedimentary rocks. In: Low Temperature Metamorphism, M. Frey (Ed.), Blackie, Glasgow and London, 9-58

Gat, J.R., Shemesh, A., Tziperman, E., Hecht, A., Georgopoulus, D., Basturk, O. 1996. The stable isotope composition of waters of the eastern Mediterranean Sea. *Journal of Geophysical Research*, 101, 6441–6451.

Gökdeniz, S. 1981. Recherches géologigues dans les Taurus Occidentales enter Karaman et Ermenek, Turquie. Les series a "tuffites vertes" Triasiques: Univérsite de Paris Sud, C.d'Orsay, These, 202 p.

Göncüoğlu, M.C. 2010. Türkiye Jeolojisine Giriş: Alpin ve Alpin Öncesi Tektonik Birliklerin Jeodinamik Evrimi. Maden Tetkik ve Arama Genel Müdürlüğü, Monografi Serisi No: 5, 69 p.

Göncüoğlu, M.C., Dirik, K., Kozlu, H. 1997. General Characteristics of pre-Alpine and Alpine Terranes in Turkey: Explanatory notes to the terrane map of Turkey. *Annales Geologique de Pays Hellenique*, 37, Geological Society of Greece, 515-536.

Graciansky, P.C. 1968. Teke Yarımadası (Likya) Torosları'nın üst üste gelmiş ünitelerinin stratigrafisi Dinaro-Toroslar'daki yeri. *Bulletin of Min. Res. and Exp.,* 71, 73-92.

Gromet, L.P., Dymek, R.F., Haskin, L.A., Korotev, R.L. 1984. The "North American shale composite": Its compilation, major and trace element characteristics. *Geochimica et Cosmochimica Acta*, 48, 2469-2482.

Guggenheim, S., Bain, D.C., Bergaya, F., Brigatty, M.F., Drits, A., Eberl, D.D., Formoso, M.L.L., Galan, E., Merriman, R.J., Peacor, D.R., Stanjek, H., Watanabe, T. 2002. Report of the AIPEA nomenclature committee for 2001: order, disorder and crystallinity in phyllosilicates and the use of the "Crystallinity Index". *Clay Minerals*, 37, 389-393.

Gutnic, M., Monod, O. 1970. Un série Mésozoique condansée dans les nappes du Taurus Occidentale, la seri edu Boyalı Tepe. C.R., Somm., *Société Géologique de France*, 5, 166-167.

Gutnic, M., Poisson, A., Dumont, J.F. 1979. Géologie des Taurides Occidentales (Turquie). Société Géologique de France, Nouvelle Série, Mémoire, 58, 112 p.

Haskin, L.A., Haskin, M.A., Frey, F.A., Wildeman, T.R. 1968. Relative and absolute terrestrial abundances of the rare earths. In: Origin and Distribution of the Elements, L.H.Ahrens (ed.). Pergamon Press, 889-912.

Hoffman, J., Hower, J. 1979. Clay mineral assemblages as low grade metamorphic geothermometers: Application to the thrust faulted disturbed belt of Montana, USA. In: Aspects of Diagenesis, P.A. Scholle and P.R. Schluger (eds.), Society of Economic Paleontologists Mineralogists Special Publication, 26, 55-79.

Hunziker, J.C., Frey, M., Clauer, N., Dallmeyer, R.D., Freidrischen, H., Flehmig, W., Hochstrasser, K., Roggwifler, P., Schwander, H. 1986. The evolution of illite to muscovite: Mineralogical and isotopic data from the Glarus Alps, Switzerland. Contributions to Mineralogy and Petrology, 92, 157 -180.

Inoue, A. 1985. Chemistry of corrensite: a trend in composition of trioctahedral chlorite/smectite during diagenesis. *Journal of College of Arts and Sciences*, Achiba University, B-18, 69-82.

Inoue, A. 1987. Conversion of smectite to chlorite by hydrothermal and diagenetic alterations, Hokuroku Kuroko mineralization area, Northeast Japan. Proc. of Int. Clay Conf., Denver. Eds. L.G. Schultz, H.van Olphen, F.A.Mumpton. The Clay Minerals Society, Bloomington, Indiana, 158-164.

Inoue, A., Utada, M., Nagata, H., Watanabe, T. 1984. Conversion of trioctahedral smectite to interstratified chlorite smectite in Pliocene acidic pyrclastic sediments of the Ohyu District, Akita Prefecture, Japan. *Clay Science*, 6, 103-116.

Inoue, A., Kohyama, N., Kitagawa, R., Watanabe, T. 1987. Chemical and morphological evidence for the conversion of smectite to illite. *Clays and Clay Minerals*, 35, 111-120.

Inoue, A., Utada, M. 1991. Smectite-to-chlorite transformation in thermally meta-morphosed volcanoclastic rocks in the Kamikita area, Northern Honshu, Japan. *American Mineralogist*, 76, 628-640.

J.C.P.D.S. (Joint Committee on Powder Diffraction Standards), 1990. Powder Diffraction File. Alphabetical Indexes Inorganic Phases. Swarthmore, United States of America, 871 p.

Kisch, H.J. 1980. Illite crystallinity and coal rank associated with lowest-grade metamorphism of the Taveyanne greywacke in the Helvetic zone of the Swiss Alps. *Eclogae Geologicae Helvetiae*, 73, 753-777.

Kisch, H.J. 1981. Coal rank and illite crystallinity associated with the zeolite facies of Southland and the pumpellyite-bearing facies of Otago, southern New Zealand. *N.Z.J. Geol. Geophys*., 24, 349-360.

Kübler B. 1968. Evaluation quantitative du métamorphisme par la cristallinité de l'illite. *Bulletin-Centre de Recherches Pau*-SNPA, 2, 385-397.

Kübler, B., Martini, J., Vuagnat, M. 1974. Very low grade metamorphism in the Western Alps. Schweiz. Mineral. Petrogr. Mitt. 54, 461-469.

Liou, J.G., Maruyama, S., Cho, M. 1987. Very low grade metamorphism of volcanic and volcanoclastic rocks-mineral assemblages and mineral facies. In Low Temperature Metamorphism. Ed. Frey, M., Blackie, Glasgow and London, 59-113.

Lippmann, F., Rothfuss, H. 1980. Tonminerale in Taveyannaz-Sandsteinen. *Schweizerische Mineralogische und Petrographische Mitteilungen*, 60, 1-29.

Marcoux, J. 1978. A scenario for the birth of a new oceanic realm: The Alpine Neotethys. Abstract, 10. International Congress on Sedimentology, Jerusalem, 2, 419-420.

Merriman R.J., Frey M. 1999. Patterns of very low-grade metamorphism in metapelitic rocks. In: Low Grade Metamorphism, M. Frey and D. Robinson (Eds.), Blackwell Sciences Ltd., Oxford, 61-107

Merriman R.J., Peacor D.R. 1999. Very low-grade metapelites: mineralogy, microfabrics and measuring reaction progress. In: Low Grade Metamorphism, M. Frey and D. Robinson (Eds.), Blackwell Sciences Ltd., Oxford, 10-60.

Merriman, R.J., Roberts, B., Peacor, D.R. 1990. A transmission electron microscopy study of white mica crystallite size distribution in a mudstone to slate transitional sequence, North Wales, UK. *Contributions to Mineralogy and Petrology*, 106, 27-44.

Monod, O. 1977. Recherches géologiques dans le Taurus occidental au sud de Beyşehir (Turquie). These, Université Paris-Sud, Orsay, 442 p.

M.T.A. (Maden Tetkik ve Arama), 2002. 1:500.000 scaled Geological Map of Turkey. *General Directorate of Mineral Research and Explorati*on, Ankara.

O'Neil, J.R. 1986. Terminology and standards, In: Stable Isotopes in High Temperature Geological Processes, J.W. Valley, H.P. Taylor and J.R. O'Neil (Eds.), *Mineralogical Society of America*, Chelsea, 561-570.

Özgül, N. 1971. Orta Torosların kuzey kesiminin yapısal gelişiminde blok hareketlerinin önemi. *Bulletin of the Geological Society of Turkey*, 14, 75-87.

Özgül, N. 1976. Torosların bazı temel jeoloji özellikleri. *Türkiye Jeoloji Kurumu Bülteni*, 19, 65-78.

Özgül, N. 1984. Stratigraphy and tectonic evolution of the Central Taurides. International Symposium on the Geology of Taurus Belt, Ankara, O. Tekeli and M.C. Göncüoğlu (Eds.), 77-90,

Özgül, N. 1997. Bozkır-Hadim-Taşkent (Orta Toroslar'ın kuzey kesimi) dolaylarında yer alan tektono-stratigrafik birliklerin stratigrafisi. *Bull. of Min. Res. and Exp.*, 119, 117-174.

Özgül, N., Arpat, E. 1973. Structural units of the Taurus orogenic belt and their continuations in neighboring regions: Selection of papers on the Eastern Mediterranean region, presented at 23rd Congress of CIESM in Athens, 1972, Bulletin *of Geological Society of Greece*, 10, 156-164.

Pettijohn, F.J. 1975. Sedimentary Rocks. Harper and Row, New York, 628 p.

Savin, S.M., Lee, M. 1988. Isotopic studies of phyllosilicates. In: Bailey, S.W. (Ed.), Hydrous Phyllosilicates. Mineralogical Society of America, Washington, DC, Reviews in Mineralogy, 19, 189–223.

Schmid, R. 1981. Descriptive nomenclature and classification of pyroclastic deposits and fragments: Recommendations of the IUGS Subcommission on the Systematics of Igneous Rocks. *Geology*, 9, 41-43.

Sheppard, S.M.F. 1986. Characterization and isotopic variations in natural waters. In: Stable Isotopes in High-temperature Geological Processes, J.W. Valley, Jr H.P. Taylor and J. O'Neil (Eds.), Mineralogical Society of America, Washington DC, *Reviews in Mineralogy*, 16, 165-184

Sheppard, S.M.F., Gilg, H.A. 1996. Stable isotope geochemistry of clay minerals. *Clay Minerals*, 31, 1-24.

Sheppard, S.M.F., Nielsen, R.L., Taylor, H.P. Jr. 1969. Oxygen and hydrogen isotope ratios of clay minerals from porphyry copper deposits. *Economic Geology*, 64, 755-777.

Srodon, J. 1984. X-ray powder diffraction identification of illitic materials. *Clays and Clay Minerals*, 32, 337-349.

Streckeisen, A. 1978. Classification and nomenclature of volcanic rocks, lamprophyres, carbonatites and melilitic rocks. IUGS Subcommission on the Systematics of Igneous Rocks. Recommendations and Suggestions. *Neues Jahrbuch für Mineralogie*, Stutgart, Abhandlungen, 31, 1-14.

Sun, S.S., McDonough, W.F. 1989. Chemical and isotopic systematics of oceanic basalts; implications for mantle composition and processes. In: Magmatism in Ocean Basins, A.D. Saunders and M.J. Norry (Eds.), *Geological Society of London, Special Publication 42*, 359-362.

Taylor, H.P., Jr. 1968. The oxygen isotope geochemistry of igneous rocks. *Contribution to Mineralogy and Petrology*, 19, 1-71.

Vergo, N., April, R.H. 1982. Interstratified clay minerals in contact aureoles, West Rock, Connecticut. *Clays and Clay Minerals*, 30, 237-240.

Weaver, C.E., Pollard, L.D. 1973. The Chemistry of Clay Minerals. *Elsevier, Amsterdam, Developments in Sedimentology 15*, 213 p.

Wenner, D.B., Taylor, H.P.Jr. 1974. D/H and O^{18}/O^{16} studies of serpentinization of ultramafic rocks. *Geochimica et Cosmochimica Acta*, 38, 1255-1286

Yalçın, H., Gümüşer, G. 2000. Mineralogical and geochemical characteristics of of Late Cretaceous bentonite deposits at the north of Kelkit valley, Northern Turkey. *Clay Minerals*, 35, 5, 807-825.

Yalçın, H., Bozkaya, Ö. 2002. Hekimhan (Malatya) çevresindeki Üst Kretase yaşlı volkaniklerin alterasyon mineralojisi ve jeokimyası: denizsuyu-kayaç etkileşimine bir örnek. C.Ü. *Mühendislik Fakültesi Dergisi Seri A-Yerbilimleri*, 19, 81-98.

Yalçın, H., Bozkaya, Ö. 2003. Sivas Batısındaki (Yıldızeli-Akdağmadeni) hidrotermal kaolin ve I-S oluşumlarının mineralojisi ve jeokimyası. *Bulletin of Turkish Association of Geology*, 46, 1-23.

Yalçın, H., Bozkaya, Ö., Tetiker, S. 2005. Kangal kömür yatağının kil mineralojisi ve jeokimyası. 12nd National Clay Symposium, Yüzüncüyıl University, Van, 5-9 September, Abstracts, 16-31.

Yeh, H.-W. 1980. D/H ratios and late-stage dehydration of shales during burial. *Geochimica Cosmochimica Acta*, 44, 341-352.